

PRESENT-DAY SEDIMENTARY FACIES IN THE COASTAL KARST CAVES OF MALLORCA ISLAND (WESTERN MEDITERRANEAN)

JOAN J. FORNÓS¹, JOAQUÍN GINÉS¹, AND FRANCESC GRÀCIA^{1,2}

Abstract: In spite of the increasing number of papers on cave sediments published during the last few decades, no one has focused from a sedimentological point of view on the processes that take place specifically within the coastal karst areas of carbonate islands. The objective of the present investigations is to deal with the sedimentary processes that take place inside two littoral caves of Mallorca (western Mediterranean), characterizing the different facies existing in the particular geological, geochemical, and hydrological setting that represents this very specific cave sedimentary environment. The recent exploration of extensive underwater galleries and chambers into some outstanding coastal caves of the island, has permitted the recognition of important accumulations of present-day sedimentary infillings in their drowned passages. Both the Pirata-Pont-Piqueta cave system and the Cova de sa Gleda have floors covered by muddy and/or sandy sediments which, in a wide sense, fit into two well-differentiated categories. On one hand we have allochthonous reddish mud sediments (mainly siliciclastic) and on the other hand autochthonous yellowish carbonate mud or sands. The mixing of both materials is also frequent as well as the accumulation of large blocks and debris due to the breakdown of roof and cave walls. A series of 21 manual cores was obtained by scuba-divers in both caves, in order to collect the full thickness of sedimentary fill. Soil samples at the entrance of the two caves, as well as rock samples of the walls of both sites, were also obtained for a later comparison. Several sedimentary facies can be distinguished, which include coarse-grained deposits (entrance facies and breakdown blocks), fine-grained siliceous sediments (silts and muddy deposits with very variable organic matter content), carbonate deposits composed of calcite raft accumulations and/or weathering-released limestone grains, and mixed facies including diverse proportions of the other sediment types. There are also some relict deposits composed of siliceous red silts, which are affected by polygonal desiccation cracks. In all the cases, the siliciclastic elements (quartz and feldspars, mainly) are related to rain events supplying dust of Saharan origin. The deposits and facies described herein correspond to different sedimentary environments that can be individualized inside the caves (collapse entrances, breakdown chambers, fully drowned passages and chambers, pools with free water surface...), and reflect very specific hydrological, geochemical, and mechanical processes related to the coastal nature of the studied karst caves.

INTRODUCTION

During the last decade, there has been a great increase in speleological and karst research on Mallorca island, especially in those peripheral areas where the coastal karst attains noteworthy development. The recent explorations of extensive underwater galleries and chambers into some outstanding littoral caves of the island are particularly important (Gràcia et al., 2007a), allowing for the detailed observation and survey of some tens of kilometers of drowned passages. These investigations have permitted the recognition of the morphological characteristics of the underwater part of these caves, which exhibit an outstanding variety of present-day sedimentary infillings in most of the explored chambers and passages (Gràcia et al., 2006, 2007b).

Cave sediments have been recognized and described since scientific interest in caves began. Nevertheless, we can consider, in general, that in-depth investigations on the subject have not been performed until recently by karst researchers. When scientists realized that sediments contain both hydrogeological and paleoclimatical records, together with the development of absolute dating techniques, the study of cave sediments become one of the most interesting topics in karst literature (White, 2007). In spite of the increasing number of references on this matter, published during the last few decades, only a few are specific synthesis works dealing with the topic (Ford, 2001; Sasowsky and

¹Dept. Ciències de la Terra. Universitat de les Illes Balears, Crta. Valldemossa, km 7.5, 07122 Palma (Balearic Islands), joan.fornos@uib.es; jginésgracia@yahoo.es

²Grup Nord Mallorca, Federació Balear d'Espeleologia, xescgracia@yahoo.es

Myroie, 2004). In the meantime, there have also appeared some general texts that include reviews of current understanding of its hydrological and geomorphological significance (Ford and Williams, 2007; Gillieson, 1996; Palmer, 2007). However, among the great number of recent papers devoted to cave sediments, no one has focused from a sedimentological point of view on the processes that take place specifically in the coastal karst areas of carbonate islands.

The flank margin model of littoral speleogenesis, developed in the Bahamas from the 1980s onwards (Myroie and Carew, 1990), recognized the importance of dissolution processes occurring in the mixing zone between fresh and sea waters, whose position is complicated by Quaternary sea-level oscillations due to glacioeustatic phenomena. This model has evolved during the 1990s until now (Myroie and Myroie, 2007) leading to the elaboration of a Carbonate Island Karst Model (CIKM), in which speleogenesis is strongly conditioned by the particular behavior of diagenetic immature (eogenetic) carbonate rocks. The CIKM progressively integrated more components into the model, taking into account both the presence and disposition of an impervious basement, if it exists, as well as the overprinting of tectonic activity and sea-level changes. Recently, Ginés and Ginés (2007) focused their work on the littoral caves of Mallorca island, adding new morphogenetic insights to the evolution of this eogenetic coastal karst. These authors particularly emphasize the role of breakdown processes, together with the recurrent glacioeustatic sea-level oscillations and the subsequent falls and rises of the water table. This cyclicity would provoke during the glacial periods the triggering of collapse by the loss of buoyant support of phreatic waters and, during the subsequent drowning associated with warm events, the underwater dissolution of boulders and collapse debris. These mechanisms will enable the enlargement of a nonintegrated array of caves and vug-porosity connected to the sea (developed in the mixing zone) rather than conventional karstic flow through conduits.

Framed into the geomorphological context above described, the objective of the present paper is to deal with the sedimentary processes that take place inside the coastal caves of Mallorca, characterizing the different facies existing in the particular geomorphological and hydrological settings that represent this very specific underground sedimentary environment. In this sense, the peculiarities of coastal karst include specific geochemical processes linked to the mixing zone (dissolution, dolomitization...) together with the decisive fact that drowning of cave passages is controlled by the sea-level position, instead of by a local base level plus the possible floods associated with events of intense recharge of the aquifer. As a consequence of its hydrogeological behavior and the low amount of precipitation, the stability of the water-table position in Mallorcan littoral areas is remarkable even at a millennial time-span, although at a longer time-scale there

were important fluctuations related to glacioeustatic variability. In general terms we are dealing with a very low energy aquatic environment, framed in a high permeability context (Upper Miocene calcarenites) without a fully karstic hydrogeological behavior: recharge is limited and dispersed, with no sinking superficial streams or flood high waters, and conduit flow is relatively less important than diffuse flow.

REGIONAL GEOLOGICAL SETTING

The two studied caves, Pirata-Pont-Piqueta system and Cova de sa Gleda, are developed in Upper Miocene limestones that crop out along the southern and eastern areas of Mallorca forming the best featured coastal karst region of the island, called Migjorn. Its littoral landscapes are characterized by significant phenomena including different types of karstic and/or marine caves, paleokarst features, littoral karren and fluvio-karstic bights or coves. The Upper Miocene limestone constitutes a post-orogenic platform that surrounds the mountain ranges (Serres de Llevant and Serra de Tramuntana) built up during the Alpine orogeny (Fig. 1). Showing a mean thickness around 70 m, that can occasionally exceed 120 m, they onlap a very irregular alpine folded and thrustured basement composed by Mesozoic dolomites and limestones with minor marl intercalations. The Upper Miocene carbonate sequence corresponds to an alternance of sedimentary bodies (Pomar, 1991) of calcilutites and very porous calcarenites, with a complex geometry, that were formed by the progradation of a Tortonian reef complex. The sequence ends with a series of carbonate tabular deposits with oolitic and mangrove facies, Messinian in age.

The Upper Miocene carbonate sequence forms a slab that stretches as a flat surface behind the coastal decametric-scale cliffs of the southern and eastern shores of the island. This characteristic tabular landscape is interrupted only by incised dry valleys filled up by Holocene sediments, ending at littoral coves whose presence and morphology are conditioned by the extensional processes occurring from the Neogene to the Quaternary. Furthermore, they were responsible for the present-day coastal morphology that is controlled by recent normal faults; also notable is a small tilting that affects the Migjorn plateau along a north-south profile and provokes the variation of sedimentary facies cropping out near the sea level.

CAVE LOCATIONS AND DESCRIPTIONS

The Pirata-Pont-Piqueta cave system is located at Can Frasquet farm-house, in the so called Marina de Manacor (Migjorn region, eastern Mallorca), near Cala Falcó small bight (UTM ED-50, 525 590/4 373 360-33) and some 0.4 km from the coast. It is composed of a series of independently explored caves that were recently connected

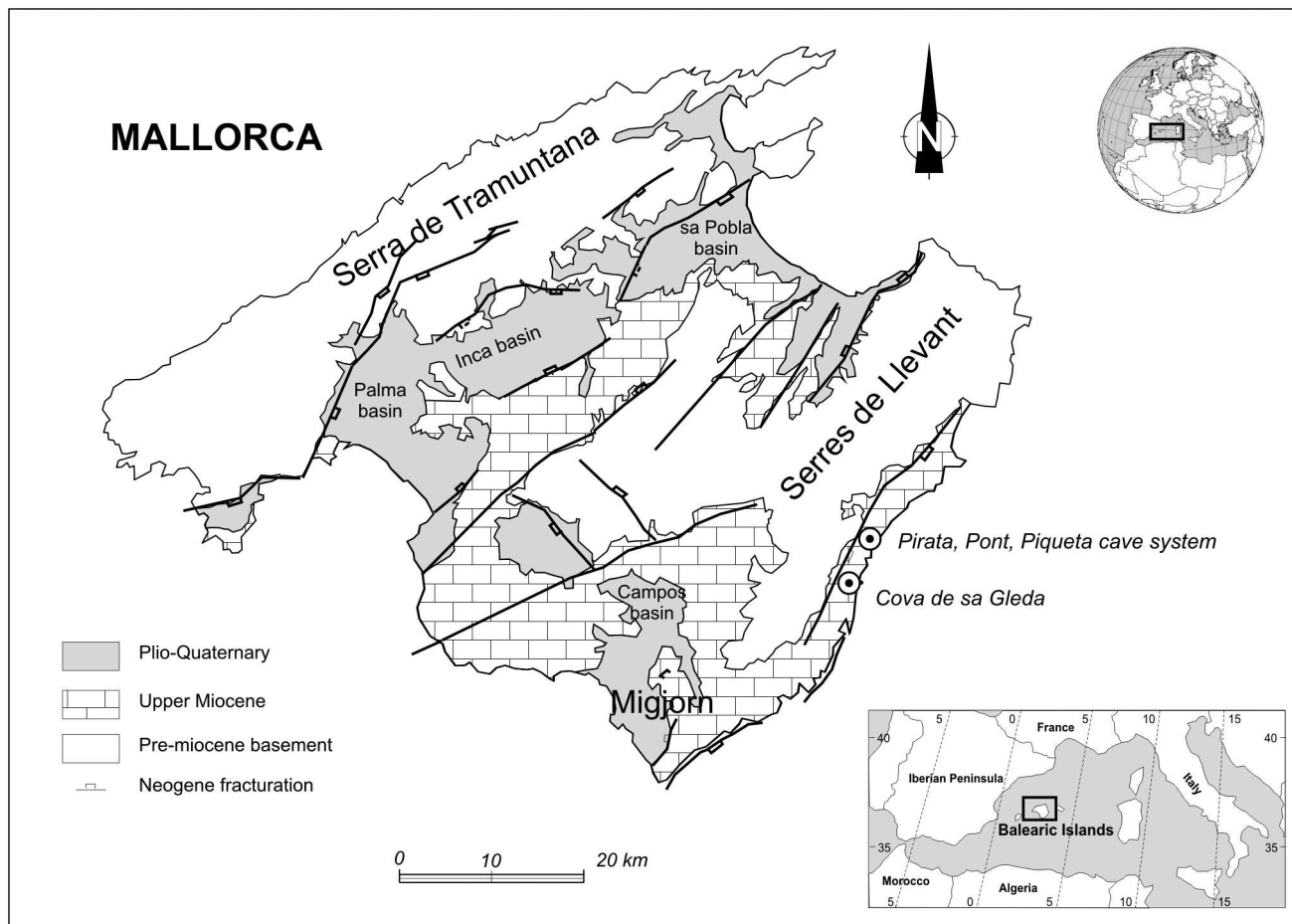


Figure 1. Geological map of Mallorca depicting the main geologic units of the island and the location of the studied caves.

by underwater exploration (Gràcia et al, 2006). The system presents a series of breakdown differentiated units, three of them corresponding to the entrance chambers. Up to date explorations include a series of chambers and galleries reaching 3,020 m of development, 1,190 m of which are underwater (Fig. 2); the surface area occupied by subterranean pools with an air surface reaches 5,000 m². Its maximum depth is 44 m, including 11 m below the present-day sea level. The passages show solution morphologies that are restricted to those sections located beneath the current phreatic level. In that sense the water column has four different well stratified water masses according to their salinity and temperature that constitute a rather complex mixing zone showing two haloclines (Gràcia et al., 2006). The linear penetration of these caves perpendicularly from the coast line is about 700 m. The speleogenesis of the system corresponds to the mixing processes between continental and marine waters that affected the Miocene calcarenites and provoked the initial void creation. Subsequent breakdown processes were induced by the glacioeustatic sea-level falls giving large block accumulations, together with spectacular speleothem ornamentation that is observed through most of the caves.

The Cova de sa Gleda is also located on the Marina de Manacor (Migjorn region) at Son Josep Nou farm-house (UTM ED-50, 523 805/4 372 315-36), 36 m above sea level and some 1.7 km from the coast. It corresponds to a subterranean complex of chambers and galleries related to some collapse sinkholes at the surface, having today a surveyed development near 10,500 m with a maximum underwater depth of 25 m (it is the largest littoral mixing-zone cave in Europe). The morphological frame of the cave shows a series of breakdown chambers (Fig. 2) which are connected to each other by phreatic galleries and passages showing circular, elliptic or irregular sections. Some of the galleries are clearly structurally controlled. The water profile in the submerged passages shows up to five different saline layers, with defined haloclines that give varied types of clearly marked corrosion morphologies (Gràcia et al., 2007b), the most interesting being the corrosion notches that affect both the cave walls and ancient speleothems formed during previous sea level low-stands. The presence of speleothems is a notable aspect of this cave. In particular, some drowned chambers and galleries show impressive precipitation morphologies forming bands of crystal coatings on the cave walls as well as on previous vadose speleothems.

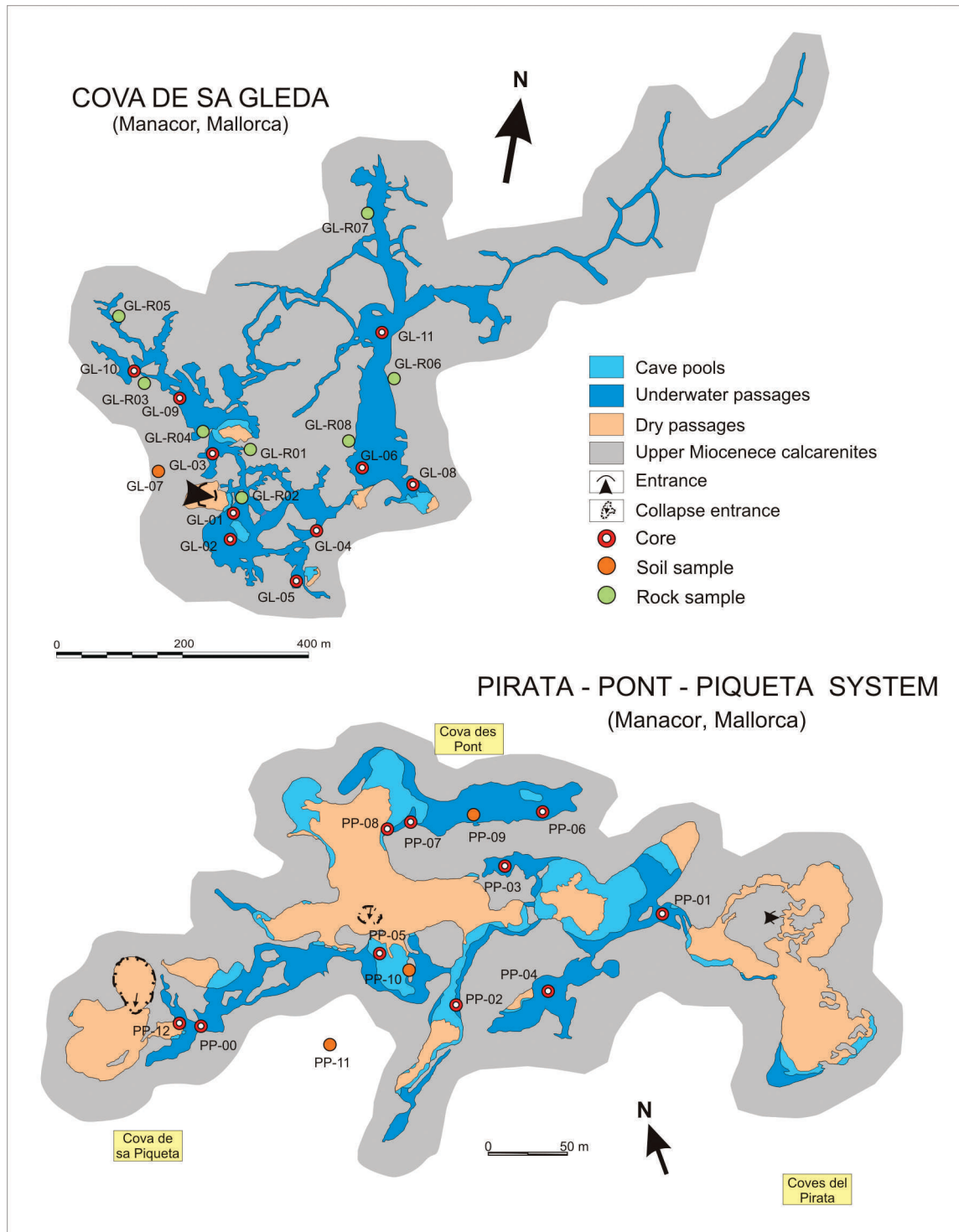


Figure 2. Cave maps of the Pirata-Pont-Piqueta system and Cova de sa Gleda (Manacor, Mallorca) showing the location of collected cores and samples. Notice that scales are different in both maps. See caves location on Fig. 1.

These bands are generated by noticeable epiaquatic carbonate precipitation, being related to previous stability levels of the water table which were in turn controlled by Quaternary sea-level oscillations (Tuccimei et al., 2006).

Both the Pirata-Pont-Piqueta cave system and the Cova de sa Gleda have important accumulations of sediments in

their chambers and passages, that are today drowned after the Holocene sea-level rise. Most of the cave floors are covered by muddy and/or sandy sediments, which in a wide sense, are marked by two well differentiated characteristics. On the one hand, we have red mud sediments (mainly siliciclastic) and on the other hand, a yellowish carbonate

mud or sand. The mixing of both materials is also frequent, as is the accumulation of large blocks and debris due to the collapse and breakdown of roof and cave walls.

METHODS

Although practically all the caves known in the eastern and southern coasts of Mallorca island show sediments in their flooded passages (Cova Genovesa [Gràcia et al., 2003]; Cova des Coll [Gràcia et al., 2005]; Cova de s'Ònix [Ginés et al., 2007]; among others), we have focused our work in only two coastal caves that are today the most representative and well known.

FIELD SAMPLE COLLECTION

A series of 20 manual cores (Fig. 2) was obtained by scuba-divers in the underwater passages of both caves (10 at Pirata-Pont-Piqueta system and 10 in Cova de sa Gleda) by introducing in the floor sediments a PVC pipe, 5.1 cm in diameter and 50-cm-long, until the full thickness of loose sedimentary fill was attained (Fig. 3). Soil samples at the entrance of the caves as well as rock samples from the walls of both caves were also obtained for subsequent comparison.

Cores obtained were bagged, sealed, numbered, and brought back to the Earth Sciences Department of the Universitat de les Illes Balears, where they were opened, longitudinally sectioned, photographed, and sampled in stratigraphic order according to the different observed levels. Samples were not taken at regular or fixed intervals due to the fact that the scope of the study was an approach to determine the different sedimentary facies existing in these littoral karst caves. Presence of sedimentary structures such as laminations and other general observations were annotated.

LABORATORY ANALYSES

A total of 136 samples (50 from Pirata-Pont-Piqueta system and 86 from Cova de sa Gleda) were sent to the laboratory where each sediment sample was air-dried for 24 hours prior to analysis. After a color description (dry and humid) using the MUNSELL soil color chart, grain-size, mineralogy, and organic matter were analyzed. Organic matter (lost on ignition [LOI]) was determined by weight loss after placing the samples in a furnace at 550 °C for three hours. Particle size distribution was determined using a Beckman Coulter-LS particle size analyzer. Cumulative curves, frequency histograms, and summary statistics were calculated.

Mineralogy was determined with a Siemens D-5000 X-ray diffractometer, using randomly oriented powders of the bulk samples. Samples were pre-treated with H₂O₂ to remove organic matter. Replicates were heated to 375 or 600 °C for 1 hour or treated with ethylene glycol at 60 °C to differentiate between clay minerals. Selected samples were analyzed by EDX (Bruker X-Falsh Detector 4020) or

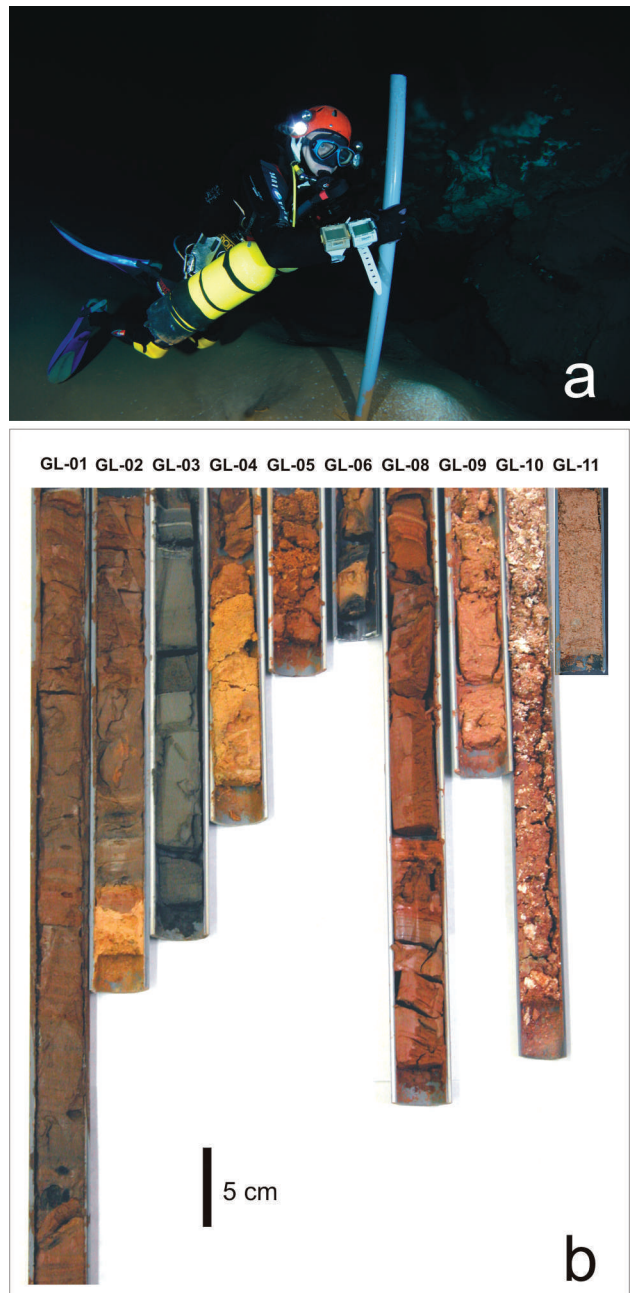


Figure 3. a) Sampling through manual coring inside the underwater passages of the caves; b) cores of sedimentary infilling from Cova de sa Gleda. See core location on Fig. 2.

observed by SEM (Hitachi® S-3400N). Semi-quantitative mineral analyses were based on the peak areas obtained using EVA ver. 7.0 software.

Radiocarbon dates were obtained from two organic debris (seeds) in order to establish a chronological frame for the studied cave sediment accumulation. The dating was performed at the Laboratoire IRPA KIK (Institut Royal du Patrimoine Artistique) of Brussels. Analyses of sampled sediments may be found on the NSS web site.

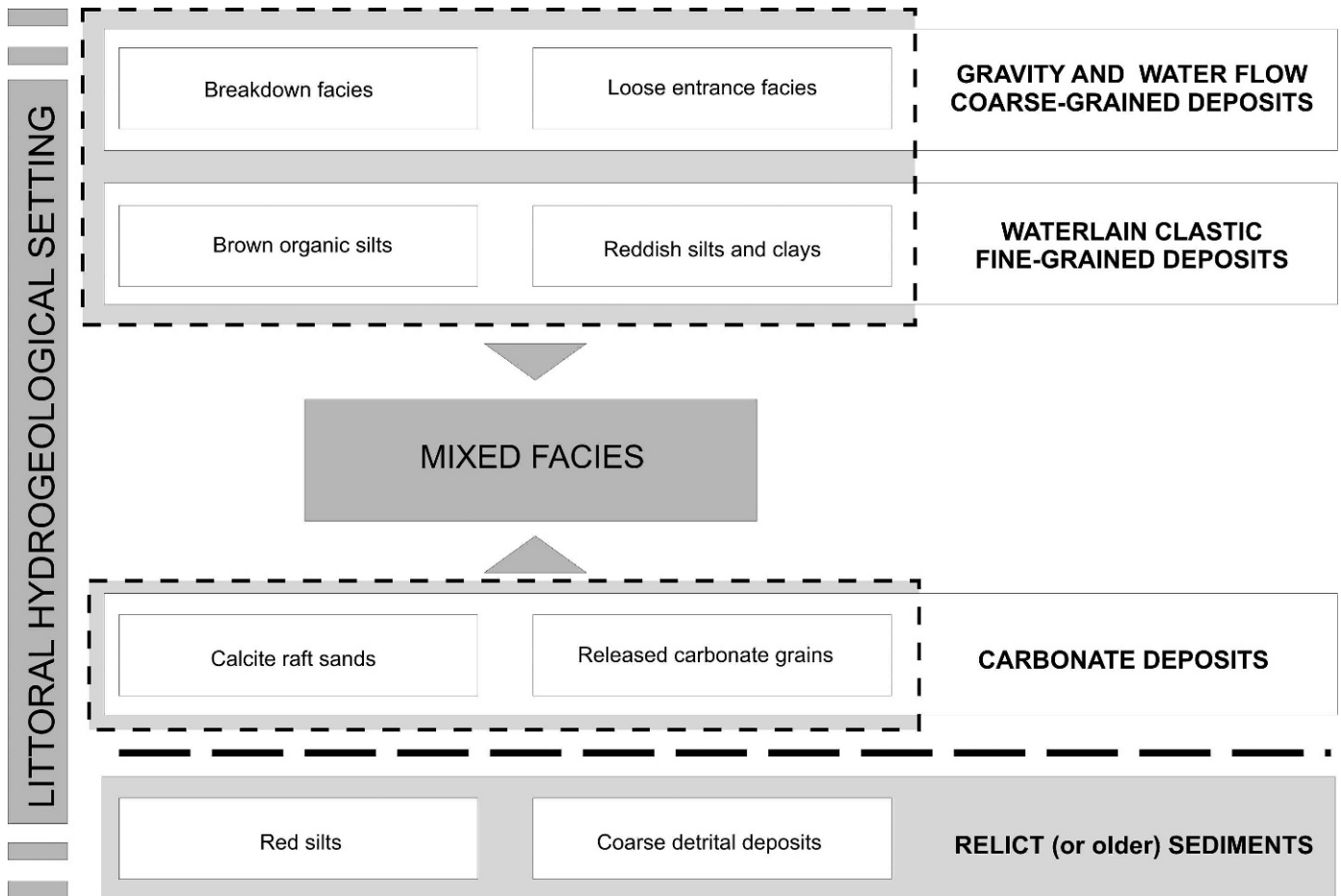


Figure 4. Sketch showing the sedimentary facies observed in the studied littoral caves.

RESULTS

Present-day sediments in the sampled caves of the Mallorcan coastal zone show accumulation thicknesses ranging between 0.5 and 1.5 m, deposited on the floors of underwater solutional galleries, small to medium in size, as well as in submerged breakdown chambers of notable dimensions. The sediments show a very irregular distribution mainly related to present or relatively recent entrances to the caves, where a light thinning trend towards the inner part of the passages can be observed. The irregular morphology of the cavities, together with the breakdown processes that affect most of the chambers, controls the thickness of the sediments.

SEDIMENTARY FACIES

In a general way we can describe the presence of red to brown siliciclastic silty and clayey sediments, pink to yellow carbonate sands, and coarse lithoclastic gravels and breccia deposits. All these deposits can be gathered into four different categories of sediments according to their textural, organic and mineralogical composition as well as their genesis: (1) Gravity and water flow coarse-grained

deposits, (2) Waterlain clastic fine-grained deposits, (3) Carbonate deposits, and (4) Relict or older deposits (Fig. 4) most of which are composed of several sedimentary facies that are forthwith described.

Gravity and Water Flow Coarse-Grained Deposits

Breakdown Facies. This facies includes unsorted boulders (ranging in size from several centimeters to near 15 m) and cobble piles with no cement binding the clasts (Fig. 5). Their composition corresponds entirely to calcarenites and, in small amount, calcisiltites coming from the Upper Miocene rocks in which the cave is located. Grain size is related to the bedding thickness of the source limestones, being usually from medium to thick (decimetric to metric) or even massive. Surface textures of the clasts are slightly weathered depending on their depth in the cave waters and the diverse geochemical behavior found there. Clasts range from sub-angular to sub-rounded depending on the textural characteristics of the original rock. Although they show a chaotic mixture regarding size and disposition, some preferred clast orientation can be observed. They are flattened in shape, according to the rock bedding, and the largest clasts show their flat sides facing parallel to the surface accumulation of

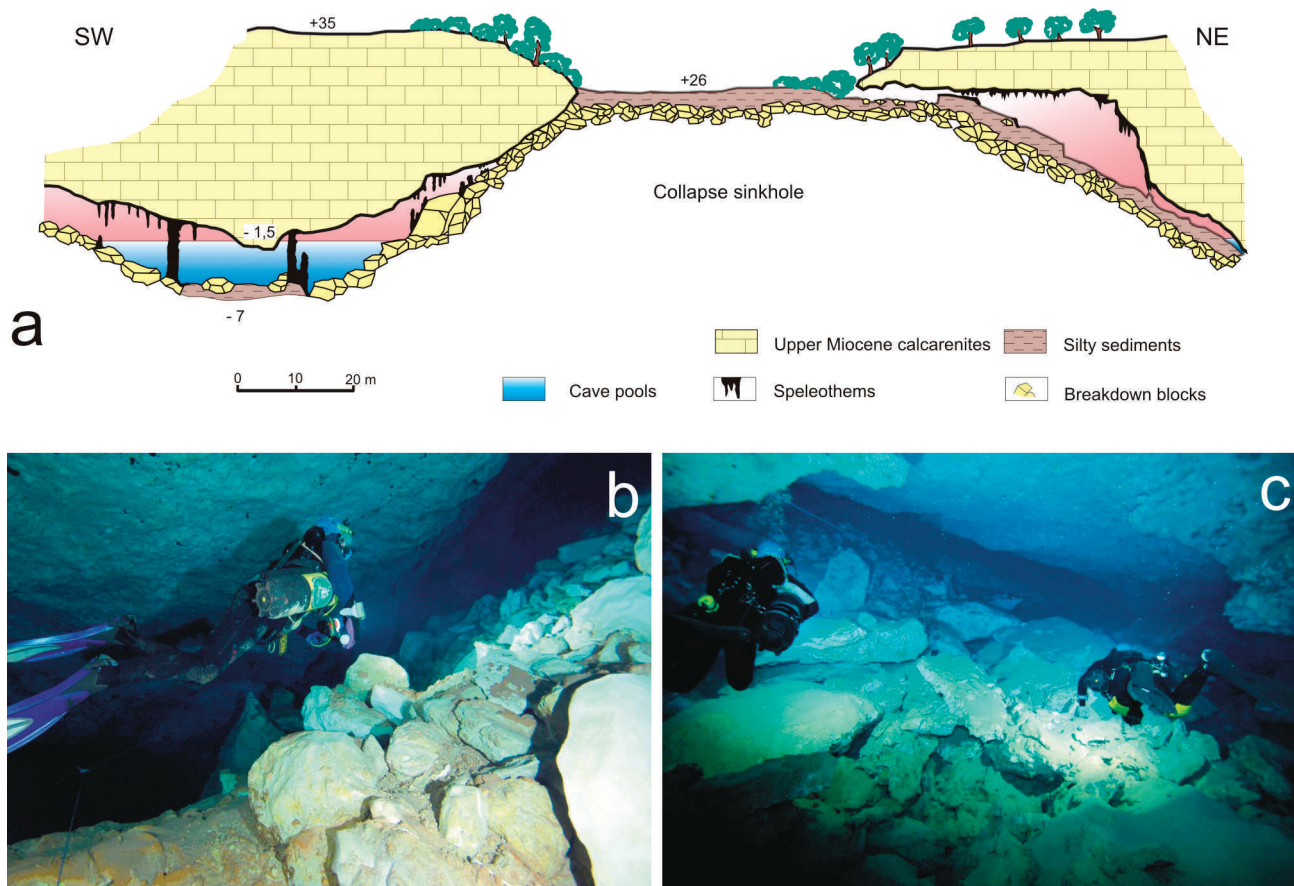


Figure 5. Pirata-Pont-Piqueta cave system, a) geomorphological section of one of the entrances with related breakdown processes; b) entrance talus deposits; c) breakdown piles due to collapse are present all around the caves.

the debris cone. The clasts don't show any imbricated structure, or any other sign of transport.

This facies corresponds to the accumulation of debris from roof as well as wall collapse, altered by solutional processes that take place in relationship to the halocline. Chip, slab or even block breakdown can be found.

Loose Entrance Facies. These deposits have some similarities to the breakdown materials previously described. Located near the current entrances or choked openings, this facies is a breccia accumulation with clasts, blocks and boulders very irregular in size and shape, mostly showing a sub-rounded morphology and having a slight inverse grading. Matrix content can be abundant and is mainly formed by silts and very fine sand coming from outside, but with a very irregular distribution. They form prograding fans usually with a high degree of slope (Fig. 5).

This facies consists of a mixing between mainly fine-grained particulate material, carried by external currents that drain to the entrance pools of the caves, and fallen fragments of rock from the cave walls. It is one of the coarsest facies present in these coastal caves, containing no well rounded sediments due to the absence of currents of sufficient strength flowing into the littoral aquifer and the

lack of allogenic currents draining to the caves. We have not observed debris flow deposits. These deposits correspond to the entrance talus of White (2007).

Waterlain Clastic Fine-Grained Deposits

Brown Organic Silts. The brown organic silts facies is one of the most extensive found in the caves, and it presents variable thicknesses ranging from 0.2 m to nearly 1 m. This facies is especially represented in the chambers and galleries with openings to the surface. They correspond to silt with low proportions of clay (around 10%) and fine sands (less than 5%). With a moderate sorting, they have a mean grain size corresponding to coarse silt and a median (D50) of fine silt (Fig. 6). Samples taken in the sediment cores show a dark reddish brown color (5YR3/4) when moist and reddish yellow (7.5YR6/6) when dried in the laboratory. The most conspicuous feature of these sediments is the presence of very fine laminations clearly defined by the alternation of reddish-brown and black laminae (Fig. 7). These millimeter-scale black laminae show a notable accumulation of vegetal fibers and seeds. The median organic content of the facies is slightly higher than 5% (LOI). From the point of view of their mineralogy it can be considered basically siliceous, with a high proportion of

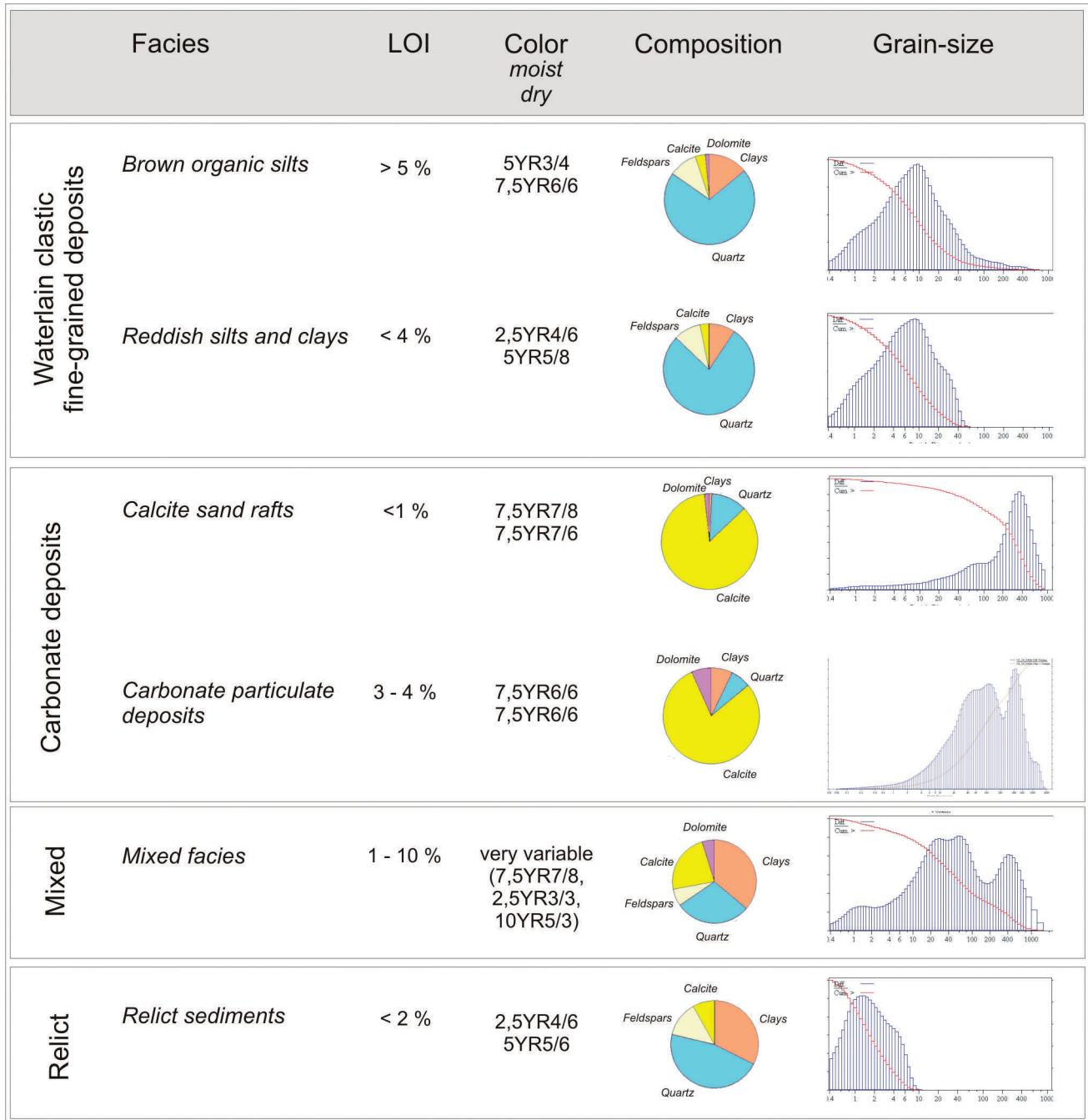


Figure 6. LOI (lost on ignition) percentage, color, mineralogical composition, and texture of the sedimentary facies described.

quartz (more than 65%), clay minerals (around 20%) and feldspars (near 10%). Carbonates (mainly calcite) are present in very low proportions (less than 5%).

The sediments that correspond to this facies are accumulated mainly in those pools and underwater passages that are located nearest the great collapse entrances to the caves. Sediment composition corresponds to soil materials transported inside the caves by flowing rain water, especially during storm events. Their composition has been traditionally related to allochthonous

siliciclastic components supplied by rains carrying down dust particles of Saharan origin (Fiol et al., 2005, Goudie and Middleton, 2001). The clear laminations due to the periodic accumulation of organic matter, including abundant vegetal fibers and seeds, are related to each one of the successive storm events entering the cave, and may not in fact have any seasonal significance. They also do not have any relation with the varve deposits so classical in glaciated regions. Carbon-14 dating of some organic components (seeds and vegetal fibers) from cores PP-08 and GL-01

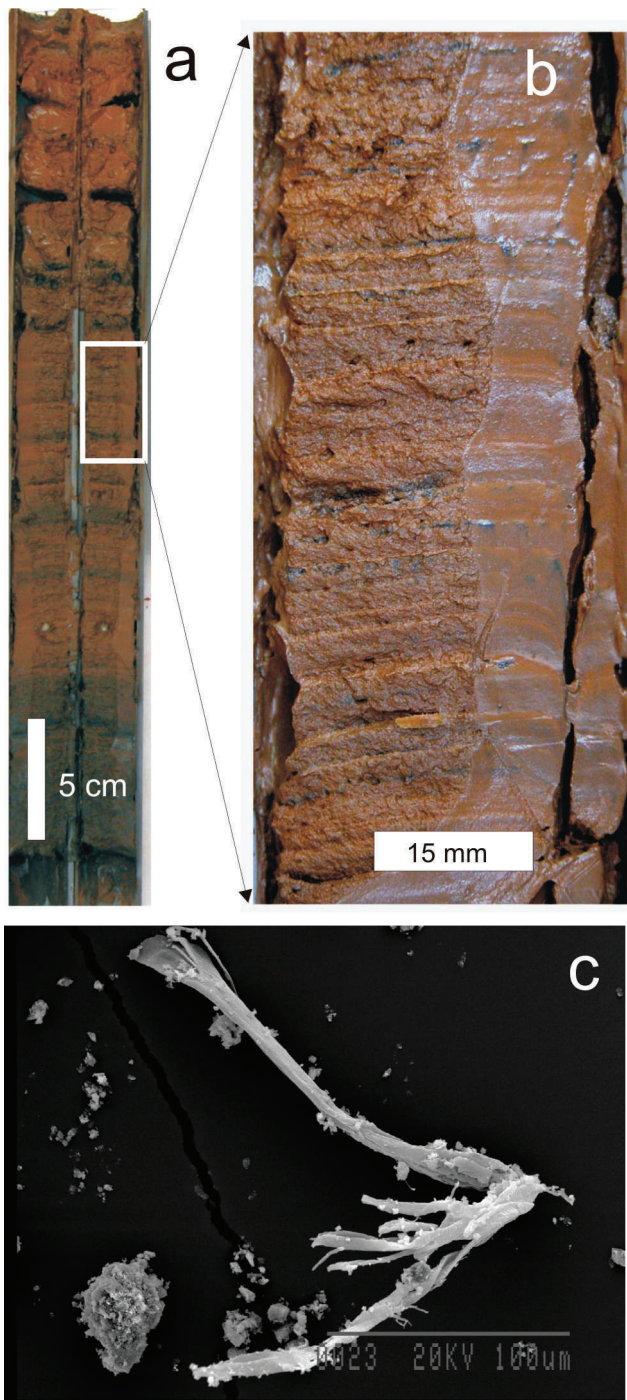


Figure 7. Brown organic silts; a) General aspect of core PP07 collected at Galeria del Llac Ras in Pirata-Pont-Piqueta cave system; b) conspicuous thin-laminations due to grain-size sorting and organic accumulation; c) vegetal fibers are the main constituents of the black laminae.

yielded ages of 220 and 330 yr BP, respectively (Fornós and Gràcia, 2007).

Reddish Silts and Clays. This facies is the least common in the studied caves, in extension as well as in thickness.

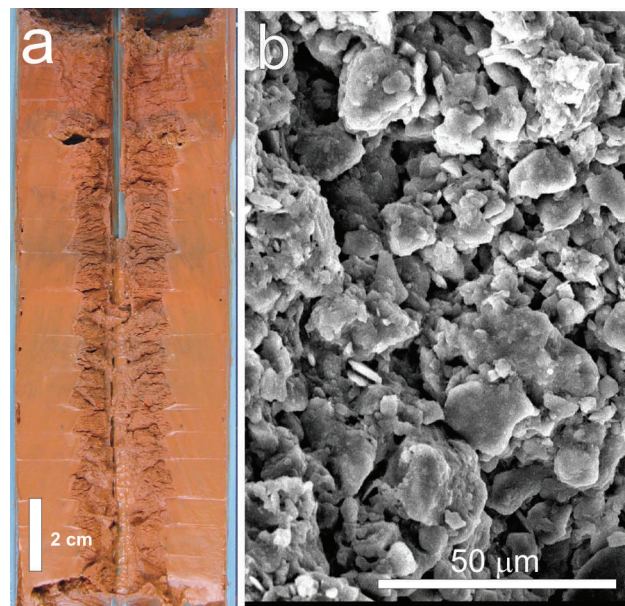


Figure 8. Reddish mud; a) core PP06 collected at the end of Galeria del Llac Ras in the Pirata-Pont-Piqueta cave system showing a massive aspect with faint lamination; b) detailed SEM image of the sediments mainly composed of quartz grains and clays.

Localized in the cores collected in the inner passages, it shows a thickness that scarcely reaches 20 cm, showing a dark red color (2.5YR4/6) when moist that transforms to yellowish red (5YR5/8) when dried in the laboratory (Fig. 8). The presence of organic matter is reduced (LOI less than 4%). Texturally (Fig. 6) the facies corresponds to silt (81%) with a small proportion of clay fraction (19%). The sand fraction is absent. It shows good sorting. Their mineralogical composition is formed of siliceous minerals with quartz representing more than 75%, feldspars with more than 10%, and clay minerals that practically never reach 10%. Presence of carbonate minerals is very low (mainly calcite with less than 3%).

Being restricted to the inner part of the caves, far away from the main entrances as well as in places with limited connections with the surface, this facies represents the fine-grained sediments that can be transported as suspended load deep into the cave system. As in the case of the organic brown silts facies, the muddy reddish silts are integrated by abundant allochthonous silicic sediments related to dust rains coming from Africa, which were progressively accumulated into the soil mantle.

Carbonate Deposits

Calcite Raft Sands. The thickness of this facies varies from a few centimeters to more than 40 cm in the sampled chambers. The sand deposits show a reddish yellow color (7.5YR7/8 moist to 7.5YR7/6 dry). Bedding is poorly defined by the existence of sub-millimeter scale horizontal

lamination resulting from the subtle presence of red muddy particles. Texture is moderately sorted and clearly dominated by the sands (> 78%) with small amounts of silts representing slightly more than 18%, and some clay (less than 3%). Thin limestone angular particles are scarce. Mean grain-size as well as the median value correspond to the transition from fine to medium sand size (Fig. 6). The organic content is very low (LOI less than 1%). Grain mineralogy is dominated by a carbonate composition with calcite (> 85%) and some dolomite (< 2%); the rest corresponds to quartz (12%) and scarce clay minerals (< 1%).

Sand grains are constituted of composite rhombohedral calcite crystals showing a clear differential geometric growth that starts with microsparite crystals, forming a planar surface that coincides with the surface of the water, and evolves to sparite crystals inside the water pool. Most of the composite crystals sand grains when found on the bottom of the pools present clear corrosion morphologies related to the geochemical processes (aggressiveness linked to the haloclines) occurring through the water column (Fig. 9).

This kind of sediment is especially abundant in the bottom of those cave pools having a free water surface that allows for CO₂ degassing. This process controls the precipitation of calcite rafts at the surface of the pools where they are maintained floating by means of surface tension, until some external process or their own growth triggers their sinking and a final accumulation at the bottom of the pool.

Carbonate Grains Released by Physico-Chemical Weathering of Limestone Walls. Thickness of this sediment facies is very variable, ranging from a few centimeters to nearly 20 cm, with distribution mainly related to the proximity to the base of cave walls or rock protuberances in general. Color is consistently reddish yellow (7.5YR6/6). Their organic matter composition is variable with mean values of different cores ranging between 3 and 4% (LOI). The textural characteristics are also quite variable, usually giving bimodal curves and showing very poor sorting (Fig. 6). The mean grain size corresponds to the fine sand fraction and the median (D50) to very fine sand. The sand fraction represents nearly 60% of the total composition, while the silt fraction is greater than 35%; the clay fraction show values around 5%. From a mineralogical point of view, their composition is mainly carbonate. Calcite represents up to 80% and dolomite around 8%. Siliceous components are formed by quartz reaching near 7% of mean values and low percentages of clay minerals (less than 4%).

These carbonate particulate deposits are the coarsest fraction in the cave systems apart from those produced by the gravity and breakdown processes. They are mainly composed of carbonate rock particles detached from the cave walls (Fig. 10), due to the differential response to

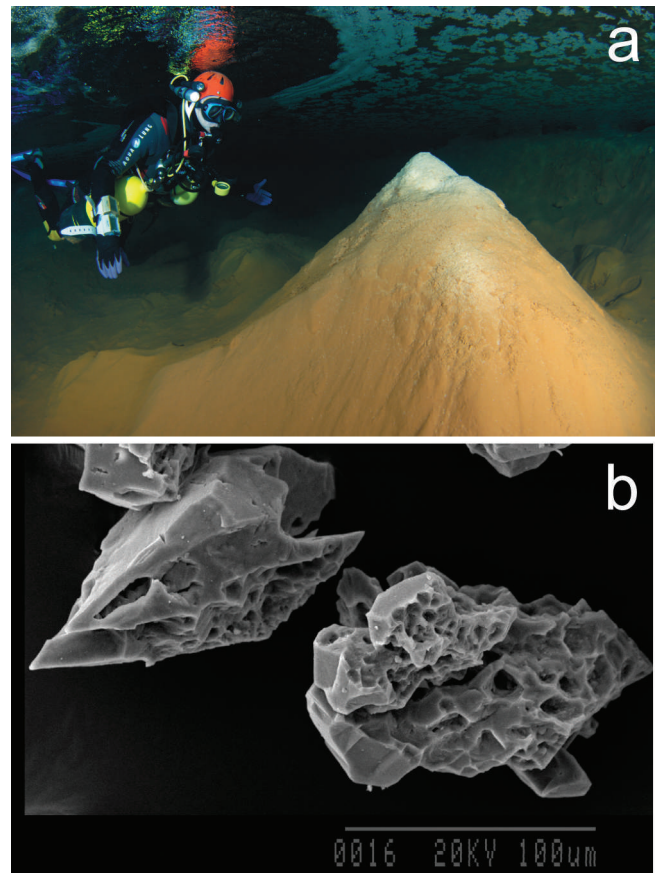


Figure 9. a) Conical structure due to the accumulation of sunken calcite rafts; b) calcite crystals corresponding to calcite rafts affected by corrosion in the mixed zone once they are sunk to the bottom of the pools.

weathering and corrosion of the variegated bioclastic grains (differing both in mineralogy and texture) that compose the enveloping calcarenite rock. This facies is particularly abundant where the current haloclines are present and carbonate grains are released by mixing corrosion.

Mixed Facies

Mixed facies are present all along the entire cave systems. They constitute a mixture of the above described facies, including both siliciclastic and carbonate sediments in different proportions (Fig. 11). The quantitative characteristics of the mixture are related to the location in the cave, presence of surface openings, depth of the drowned areas, distance to the sea, presence of pools with free air surface, etc. The resulting texture and composition differ from the end members corresponding to the different facies which have been characterized in the previous paragraphs (Fig. 6). From the mineralogical point of view, these facies also correspond to a very variable mixture of siliceous components and carbonate grains, including both crystal aggregates as well as particulate material.

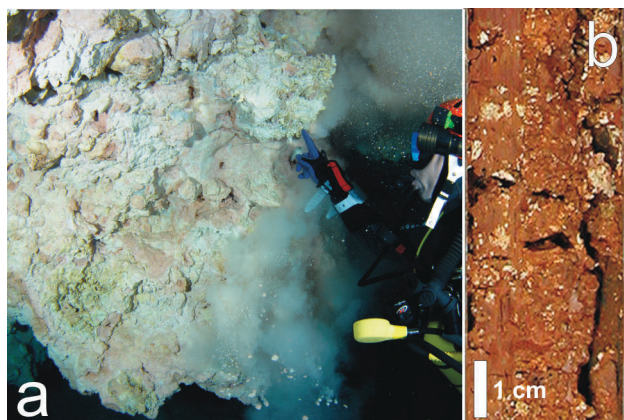


Figure 10. Incongruent corrosion of the Miocene calcarenites related to the mixing zone gives way to a granular disintegration producing abundant carbonate sediment; a) sandy grain size rain of sediment; b) core GL10 from Galeria dels Degotissos in Cova de sa Gleda showing the coarsest sediments in the cave systems, being mainly composed of heterometric carbonate rock particles.

Color is very variable embracing shades of reddish yellow (7.5YR7/8) to dusky red (2.5Y3/3) or even brown (10YR5/3). Organic matter also has a great variability, ranging from 1% to more than 10%. Usually the textural curves show bimodality and poor to very poor degrees of sorting. Mean grain size ranges from fine sand to coarse silt, while the median varies between very coarse silt to medium silt. Textural fractions show figures between 14% and 40% for sand, between 50% and 60% for silt and between 7% and 25% for the clay fraction. The mineral composition also has a great variability. Calcite ranges between more than 90% to less than 30%, dolomite from 3% to 6%, quartz from more than 40% to less than 3%; feldspars have a maximum of 10%, but can be also absent in some samples and, finally, the clay minerals range from 1% to slightly more than 10%.

Relict or Older Deposits

Red Silts. Ancient deposits composed of red silts are up to 15 cm thick in some sampled chambers. The color is dark red (2.5YR4/6) when moist and yellowish red (5YR5/6) when dry. Bedding is very poorly defined but locally there is a millimeter-scale black lamination, resulting from organic-matter concentration. On the surface of these sediments decimeter-scale mud desiccation cracks (up to 4 cm deep) are clearly visible (Fig. 12). The mean organic content (LOI) is around 2%. Texturally this facies represents a mixing of silts (52%) and clays (47%) with a very low presence of sand material (less than 1%); it shows a very good sorting. The mean grain-size corresponds to very fine silt and the median (D₅₀) lies between silt and clay fractions. Mineralogical content is dominated by quartz (> 43%) and clays (mainly illite and kaolinite with



Figure 11. Carbonate, silicic or mixed sediments presently extensively covering the floor of the caves (Galeria de les Còniques, Cova de sa Gleda).

some montmorillonite) with values above 33%. Feldspar minerals represent slightly less than 13%, calcite near 9% and dolomite 2%.

This sedimentary facies is composed of clay and silt particles that accumulate in ponded areas of passages receiving episodic slow-moving storm water input from the collapse entrances. The presence of abundant mud cracks splitting the sedimentation into polygonal blocks on the top of these red silty materials indicates a drying period occurred after the deposition of such mud by slow-moving water. The existence of mud cracks on the surface of these sediments (today located in underwater passages extending well below the sea level) clearly reflects the fact that they correspond to an early infilling of the cave linked to some Pleistocene sea-level fall, probably corresponding to the last glacial event.



Figure 12. Sediments very similar to present-day reddish mud, but presenting desiccation cracks are present in some places (-4 m, Galeria del Llac Ras, Pirata-Pont-Piqueta cave system). Their deposition must correspond to some sea-level fall event, probably to the last glaciation.

Coarse Detrital and Gravity Fallen Deposits. These materials are analogous to the coarse-grained deposits previously described (mainly gravity emplaced) but with a genesis related to previous episodes of breakdown in the cave. They are the result of autogenic breakdown processes favored by the repetitive loss of hydraulic buoyancy during Pleistocene glacial periods and the subsequent sea-level falls. Usually they are covered with a thin veil of more recent sediments, which can be found also as matrix infiltrates between the breccia clasts.

DISCUSSION

Sedimentation inside the coastal karst caves of Mallorca comprises both autochthonous and allochthonous components provided by a relatively wide diversity of geomorphic mechanisms acting in the different aquatic environments existing along the cave systems. The processes involved vary from rock collapse to fine-grained waterlain clastic sediments, including diverse mechanisms such as underwater weathering of rock surfaces, precipitation of calcite crystals, and infiltration of soil materials (Fig. 13). Investigations carried out on two of the most important coastal caves of the island have allowed the characterization of several differentiated sediment facies, which clearly correspond to specific locations within the whole cave system. The proximity to the cave entrances or blocked openings to the surface, as well as the geochemical behavior of the phreatic waters (dissolution, precipitation, etc.), is crucial in order to explain the cave sediments distribution together with the particular topography of the underwater galleries and chambers.

INTERPRETATION OF THE CAVE SEDIMENTARY RECORD

Breakdown or collapse has been one of the most invoked processes of later evolution in the development of the coastal caves of Mallorca (Gràcia et al. 2006, 2007a, 2007b). The repeated flooding and emptying of the original phreatic passages, during the Pleistocene glacio-eustatic oscillations, caused the passages to be altered in shape and dimensions by breakdown processes, especially when the caves were drained during sea-level falls, and favoring the failure of roofs and walls particularly along the bedding planes and joints (Gillieson, 1996; Ginés and Ginés, 2007). The maximum sea-level fall during the last glacial period was around 135 m below present-day datum (Lambeck and Chappell, 2001; Lambeck and Purcell, 2005); this figure, together with the rather modest depth attained by the caves (maximum 25 m below the current sea level) due to the presence of impervious facies at the base of the Miocene sequence, suggests that all the known chambers and passages had been emptied several times during the Pleistocene cold periods, favoring in that way the actuation of collapse processes.

Most of the entrances to the caves correspond to collapsed roofs that today act as collectors of some surface

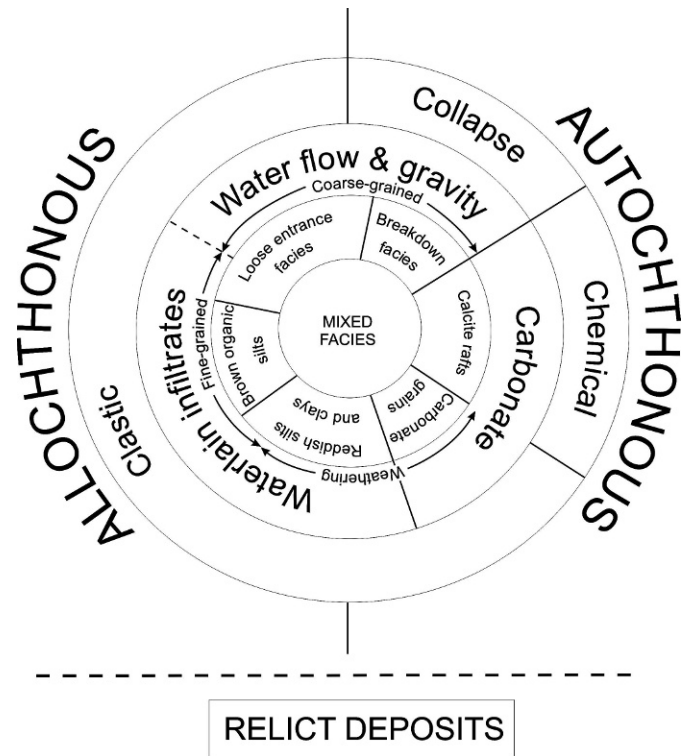


Figure 13. Sedimentary facies and involved processes in the coastal karst caves of Mallorca island.

runoff, and represent preferential sinking points that quickly drain precipitation towards the water table. Depending on the strength of the storm events and the resulting runoff, many types of sedimentary material can be transported down slope by episodic water flows. Furthermore, the processes related to the breakdown facies are also present in the cave openings, where intensive weathering of the rock walls also takes place. All these materials, as well as particles eroded from the soil, are incorporated in the loose entrance facies, and after a more or less prolonged sheet flow transport may be deposited at some cave pools near the entrances forming a delta-like architecture. Thus, loose materials can accumulate in the entrance chambers simply by gravity or by being carried in flowing water. The result is a mixing of gravels, sands, and silty material deposited in the caves by the runoff from the land surface together with weathered elements from the cave walls or ceilings as well as soil particles. The Migjorn region, where the caves are found, is an autogenic karst mantled with only a discontinuous thin soil. The catchment area is relatively minor (some square kilometers) so the volume of external detrital sediment is rather small.

Episodic water flows that enter the caves through the existing collapse openings after intense periods of rainfall, which characterize the Mediterranean weather particularly in autumn (Guijarro, 1986), transport heterometric materials until reaching the water table at the ponds inside the caves. The coarsest elements accumulate at the entrance

pools forming pseudo deltas, as have been mentioned above, while the muddy finest material is introduced inside the submerged galleries of the cave where the sedimentary accumulation takes place mostly by decantation according to the hydraulic characteristics of the water body and the grain size properties of the transported particles. Clay and silt accumulate thus in drowned inner passages where there is a slow-moving floodwater transport. The distance inside the cave that sediment can reach will depend on the geometry and morphology of the cave system and the initial impulse of the water flooding after heavy storms, as well as the interaction with the slow water movement inside the aquifer induced by the tidal (and/or barometric) sea-level oscillations. In this manner, different facies are deposited varying mainly in grain-size and organic matter content. As a result, the inner fine sedimentation is clayey and with very low organic-matter content (reddish mud facies), whereas sediments emplaced nearest the collapse openings are silty and usually show very clear black laminations of organic matter, and are related to the successive storm events that supply materials to the entrance pools (brown organic silts). Carbon-14 datings of organic components (220 and 330 yr) confirm the subactual character of these deposits.

Mineralogy of the fine-grained sediments (both brown organic silts and reddish mud) is mainly siliceous, including quartz, feldspar and clay minerals. This fact points to an allochthonous origin related to rains, coming from the south or south-east, that supply silicic dust of Saharan source; these atmospheric situations are relatively common in the western Mediterranean when a center of low pressure remains situated over the Iberian peninsula (Fiol et al., 2005). Although some of the insoluble residue from the dissolution of bedrock can contribute to the detrital sedimentation in the caves, the analysis done on the surrounding rocks shows that their non-carbonate impurities are less than 1%. Nevertheless there is a great amount of carbonate granular (sand sized) material that has been produced by the weathering and disaggregation of the bedrock, producing detached particles that are eventually accumulated simply by falling into the submerged passages and chambers. These carbonate grains are released by the differential physico-chemical weathering of limestone or dolomite from the bedrock, as well as by the different solubility of bioclastic grains according to their mineralogy and in relation to their biological composition. In that way, the production of released carbonate grains is favored owing to the incorporation of these particulate materials into the sedimentary record of the cave system. Although these processes are most typical of caves that contain little or no running water, being exposed to long-term weathering in air (Palmer, 2007), in littoral caves, as is our case, weathering in this phreatic environment can be enhanced by the geochemical activity of the coastal mixing zone.

Deposits constituted by calcite raft sands are linked to those cave pools with free water surface, that allows for

CO₂ degassing and carbonate precipitation. When these calcite rafts are sunk by dripping water, or for whatever reason, they accumulate as coarse sands of loose crystal aggregates of calcite that can reach notable thickness. When submerged and deposited in the bottom of the pools, the calcite crystals may present dissolution traces related to the geochemical processes occurring in the haloclines. The so called mixed facies are the most abundant sediments in the studied caves, being a mixture of all the previously described materials in different proportions. Grain size is normally bimodal (sand and silt fractions are predominant) and mineralogy is very diverse, including both allochthonous siliceous grains together with carbonate particles released by dissolution and/or calcite raft crystals. Their distribution and importance are very variable and depend mainly on the relationship between main entrances to the caves, presence of pools with free-air surfaces, and depth of the haloclines in the submerged galleries.

In spite of the previously discussed specificity of the coastal karst environment, most of the observed sediment types correspond in broad terms to the backswamp facies of Bosch and White (2004) because they are constituted by a variety of infiltrated soil materials, weathering residues, and carbonate precipitates having experienced very limited lateral transport. On the other hand, the reddish mud deposits present in the inner parts of the cave systems show some analogies to the slackwater facies (Bosch and White, 2004), but framed in a low-energetic context linked to the coastal karst hydrological behavior quite different from conventional stream caves.

Relict or ancient sediments are also present in the studied caves, being very similar to present-day reddish mud deposits, but showing desiccation cracks that situate their deposition in some sea-level fall event (perhaps the Last Glaciation). Mineralogy predominantly includes allochthonous siliceous grains, supplied by dust rains of African origin. An adequate interpretation of these ancient sedimentation phases will strongly benefit from the investigation of the present-day deposits from the coastal caves of the island.

CONCLUSIONS

Several main conclusions can be drawn in reference to the sedimentary processes occurring in this specific cave environment of the coastal karst system. Clastic sedimentation in the coastal caves of Mallorca island is fully conditioned by the hydrogeological specificity of the littoral karstification affecting high permeability rocks (calcarenites Upper Miocene in age). No allogenic streams are present in the Migjorn karst region, and the coastal aquifers are characterized by a rather diffuse flow to the sea. Nevertheless, an important factor in the distribution of sediment is episodic influx of meteoric water during storm events.

Several facies can be found in the cave systems, which can be grouped into gravity and waterflow coarse-grained

deposits, waterlain clastic fine-grained deposits, carbonate deposits and mixed facies. Relict deposits are also present, being related to the morphological evolution of the cave during the Pleistocene.

The diversity of represented facies is related to the topographical and geomorphological position of sampled points within the cave system. Breakdown processes of underground passages, triggered by Pleistocene sea-level oscillations, give place to collapse entrances and choked openings favoring the presence of entrance facies, and the penetration of sediments carried by runoff waters. Brown organic silt facies are particularly widespread near present-day entrances to the caves. The abundance of siliceous sediments in the fine-grained deposits must be related to dust rains of Saharan origin, which are frequent in the Western Mediterranean. Particles of carbonate material are important constituents of some deposits, in the form of rock grains released by differential dissolution weathering or sunken calcite rafts. It is very common to have the presence of mixed facies that include allochthonous siliciclastic silts and mud together with autochthonous carbonate particles. Coastal karst caves host a very specific sediment assemblage that requires increasing attention.

ACKNOWLEDGEMENTS

This work was partially supported by the research fund of Ministerio de Educación y Ciencia – FEDER, CGL2006-11242-C03-01/BTE. We thank to F. Hierro (SEM), J. Cifre (X-ray analysis), and M. Guart (grain-size analysis) for helping in lab analysis. The authors are grateful to B. Clamor, M. Febrer and P. Gamundí for their help during the field sampling and A. Ginés for their constructive comments and help in writing the manuscript.

REFERENCES

- Bosch, R.F., and White, W.B., 2004, Lithofacies and transport of clastic sediments in karstic aquifers, in Sasowsky, I.D., and Mylroie, J., eds., *Studies of cave sediments: Physical and chemical records of paleoclimate*: New York, Kluwer Academic/Plenum Publishers, p. 1–22.
- Fiol, L., Fornós, J.J., Gelabert, B., and Guijarro, J.A., 2005, Dust rains in Mallorca (Western Mediterranean): Their occurrence and role in some recent geological processes: *Catena*, v. 63, p. 64–84.
- Ford, D.C., and Williams, P.W., 2007, *Karst hydrogeology and geomorphology*: Chichester, Wiley, 561 p.
- Ford, T.D., 2001, *Sediments in caves*: Somerset, U.K., BCRA Cave Studies Series, no. 9, 32 p.
- Fornós, J.J., and Gràcia, F., 2007, Datació dels sediments recents que rebleixen les cavitats de sa Gleda i del sistema Pirata-Pont-Piqueta: *Primeres dades*: *Endins*, v. 31, p. 97–100.
- Gillieson, D., 1996, *Caves. Processes, Development, Management*: Cambridge, Blackwell Publishers, 324 p.
- Ginés, A., and Ginés, J., 2007, Eogenetic karst, glacioeustatic cave pools and anchialine environments on Mallorca Island: A discussion of coastal speleogenesis: *International Journal of Speleology*, v. 36, no. 2, p. 57–67.
- Ginés, J., Fornós, J.J., Trias, M., Ginés, A., and Santandreu, G., 2007, Els fenòmens endocàrstics de la zona de ca n'Olesa: la cova de s'Ònix i altres cavitats veïnes (Manacor, Mallorca): *Endins*, v. 31, p. 5–30.
- Goudie, A.S., and Middleton, N.J., 2001, Saharan dust storms: Nature and consequences: *Earth-Science Reviews*, v. 56, no. 1–4, p. 179–204.
- Gràcia, F., Clamor, B., Fornós, J.J., Jaume, D., and Febrer, M., 2006, El sistema Pirata-Pont-Piqueta (Manacor, Mallorca): *Geomorfologia, espeleogènesi, hidrologia, sedimentologia i fauna*: *Endins*, v. 29, p. 25–64.
- Gràcia, F., Clamor, B., Jaume, D., Fornós, J.J., Uriz, M.J., Martín, D., Gil, J., Gràcia, P., Febrer, M., and Pons, G., 2005, La cova des Coll (Felanitx, Mallorca): *Espeleogènesi, geomorfologia, hidrologia, sedimentologia, fauna i conservació*: *Endins*, v. 27, p. 141–186.
- Gràcia, F., Fornós, J.J., and Clamor, B., 2007a, Cavitats costaneres de les Balears generades a la zona de mescla, amb importants continuacions subaquàtiques, in Pons, G.X., and Vicens, D., eds., *Geomorfologia Litoral i Quaternari. Homenatge a Joan Cuerda Barceló*. *Mon. Soc. Hist. Nat. Balears*, v. 14, p. 299–352.
- Gràcia, F., Fornós, J.J., Clamor, B., Febrer, M., and Gamundí, P., 2007b, La cova de sa Gleda I. Sector Clàssic, Sector de Ponent i Sector Cincents. (Manacor, Mallorca): *Geomorfologia, espeleogènesi, sedimentologia i hidrologia*: *Endins*, v. 31, p. 43–96.
- Gràcia, F., Jaume, D., Ramis, D., Fornós, J.J., Bover, P., Clamor, B., Gual, M.A., and Vadell, M., 2003, Les coves de Cala Anguila (Manacor, Mallorca). II: La Cova Genovesa o Cova d'en Bessó. *Espeleogènesi, geomorfologia, hidrologia, sedimentologia, fauna, paleontologia, arqueologia i conservació*: *Endins*, v. 25, p. 43–86.
- Guijarro, A., 1986, *Contribución a la bioclimatología de las Baleares* [Ph.D. thesis]: Palma de Mallorca, Universitat de les Illes Balears, 232 p.
- Lambeck, K., and Chappell, J., 2001, Sea level change through the Last Glacial Cycle: *Science*, v. 292, no. 5517, p. 679–686.
- Lambeck, K., and Purcell, A., 2005, Sea-level change in the Mediterranean Sea since the LGM-. Model predictions for tectonically stable areas: *Quaternary Science Reviews*, v. 24, p. 1969–1988.
- Mylroie, J.E., and Carew, J.L., 1990, The flank margin model for dissolution cave development in carbonate platforms: *Earth Surface Processes and Landforms*, v. 15, p. 413–424.
- Mylroie, J.R., and Mylroie, J.E., 2007, Development of the carbonate island karst model: *Journal of Cave and Karst Studies*, v. 69, no. 1, p. 59–75.
- Palmer, A.N., 2007, *Cave Geology*: Dayton, Cave Books, 454 p.
- Pomar, L., 1991, Reef geometries, erosion surfaces and high-frequency sea-level changes, Upper Miocene Reef Complex, Mallorca, Spain: *Sedimentology*, v. 38, p. 243–269.
- Sasowsky, I.D., and Mylroie, J., eds., 2004, *Studies of cave sediments. Physical and Chemical Records of Paleoclimate*: New York, Kluwer Academic/Plenum Publishers, 329 p.
- Tuccimei, P., Ginés, J., Delitala, M.C., Ginés, A., Gràcia, F., Fornós, J.J., and Taddeucci, A., 2006, Last interglacial sea level changes in Mallorca island (western Mediterranean). High precision U-series data from phreatic overgrowths on speleothems: *Zeitschrift für Geomorphologie N.F.*, v. 50, no. 1, p. 1–21.
- White, W.B., 2007, Cave sediments and paleoclimate: *Journal of Cave and Karst Studies*, v. 69, no. 1, p. 76–93.

APPENDIX I

Table 1. Sample color, in dry and wet conditions, and LOI of sediments present at Pirata-Pont-Piqueta System.

Core	Sample Number	Depth (cm)	Color		LOI (%)
			moist	dry	
PP-00	01	0–2.5	5YR4/6	–	–
	02	2.5–4	7.5YR6/8	–	–
PP-01	01	0–3	2.5YR5/8	7.5YR6/6	6.27
	02	3–9	7.5YR5/8	7.5YR7/6	5.08
	03	9–15	7.5YR5/8	7.5YR7/6	6.60
	04	15–20	2.5YR3/6	7.5YR5/8	3.11
	05	20–26	2.5YR3/6	7.5YR5/8	2.37
PP-02	01	0–3	7.5YR5/8	7.5YR7/6	7.63
	02	3–3.5	5YR4/6	7.5YR6/6	2.86
	03	3.5–7	7.5YR5/8	7.5YR7/6	3.89
	04	7–13.5	7.5YR6/8	7.5YR8/4	3.34
	05	13.5–21	7.5YR6/6	10YR7/6	2.52
	06	21–23	7.5YR7/6	7.5YR8/4	2.77
	07	23–25	7.5YR6/6	–	–
PP-03	01	0–3	2.5YR3/3	7.5YR5/6	4.34
PP-04	01	0–4	5YR4/6	7.5YR6/6	1.76
	02	4–9	5YR4/6	7.5YR6/6	1.90
PP05	01	0–7	2.5YR4/6	7.5YR5/6	4.07
	02	7–13	2.5YR4/6	7.5YR5/6	3.39
	03	13–16	2.5YR4/6	7.5YR6/6	3.07
	04	16–21	2.5YR4/6	7.5YR6/6	3.41
PP-06	01	0–3	2.5YR4/6	5YR5/8	2.24
	02	3–5	2.5YR4/8	5YR5/8	2.44
	03	5–7.5	2.5YR4/6	5YR5/6	3.49
	04	7.5–11	2.5YR4/8	5YR5/6	3.07
	05	11–16	2.5YR4/8	5YR5/6	2.07
PP-07	01	0–3	2.5YR3/6	7.5YR5/6	3.97
	02	3–7	2.5YR3/6	7.5YR5/6	3.31
	03	7–9.5	2.5YR3/4	7.5YR6/6	2.80
	04	9.5–12.5	5YR3/3	7.5YR6/6	4.60
	05	12.5–16.5	5YR3/4	7.5YR6/6	4.69
	06	16.5–19.5	5YR3/4	7.5YR6/6	4.66
	07	19.5–20.5	5YR3/4	7.5YR6/6	5.17
	08	20.5–22.5	5YR3/3	7.5YR5/4	4.43
	09	22.5–26	5YR2.5/2	7.5YR5/4	3.91
	10	26–34	5YR2.5/1	7.5YR6/4	4.09
PP-08	01	0–3.5	2.5YR4/4	5YR5/6	5.26
	02	3.5–6	2.5YR4/6	7.5YR5/6	5.15
	03	6–12.5	2.5YR4/6	5YR5/8	4.65

Table 1. Continued.

Core	Sample Number	Depth (cm)	Color		LOI (%)
			moist	dry	
PP-08bis	04	12.5–17.5	5YR3/4	7.5YR5/6	4.55
	05	17.5–25.5	5YR3/4	7.5YR5/6	4.74
	06	25.5–27.5	5YR3/4	7.5YR5/6	4.20
	07	27.5–32	5YR3/4	7.5YR5/6	5.22
	08	32–37	5YR3/3	7.5YR5/6	4.77
	09	37–45	7.5YR3/2	7.5YR5/6	7.06
PP-09	10	45–53	10YR3/3	7.5YR5/4	7.59
	11	53–62	10YR3/3	7.5YR6/4	6.81
PP-11	01	0–10	2.5YR4/8	5YR5/6	4.45
PP-12	01	surface	7.5YR4/6	5YR4/6	12.50
	01	0–10	7.5YR7/8	7.5YR7/6	1.09
	02	10–20	7.5YR7/8	7.5YR7/4	1.36
	03	20–30	7.5YR7/8	7.5YR7/6	1.18
	04	30–40	7.5YR7/8	7.5YR8/4	1.53

Table 2. Sample color, in dry and wet conditions, and LOI of sediments present at Cova de sa Gleda passages.

Core	Sample Number	Depth (cm)	Color		LOI (%)
			moist	dry	
GL-01	01	0–5.5	2.5YR4/8	7.5YR6/4	9.43
	02	5.5–13	5YR4/6	7.5YR6/4	9.39
	03	13–17	5YR4/3	7.5YR6/6	9.80
	04	17–21	7.5YR3/3	10YR5/4	9.59
	05	21–26.5	7.5YR3/4	7.5YR6/3	11.03
	06	26.5–30	10R4/8	7.5YR5/6	9.34
	07	30–36	2.5R4/4	7.5YR6/4	9.85
	08	36–39	5YR3/3	10YR5/4	9.68
	09	39–43.5	5YR3/3	7.5YR5/4	9.86
	10	43.5–46	5YR3/2	7.5YR5/4	10.91
	11	46–50	5YR3/3	10YR4/4	10.99
	12	50–51.8	2.5YR4/6	–	–
	13	51.8–52.5	2.5YR5/8	7.5YR5/6	10.03
	14	52.5–56.5	2.5YR4/6	7.5YR5/4	9.55
	15	56.5–60	7.5YR3/4	7.5YR5/6	9.35
GL-02	01	0–4	2.5YR4/6	7.5YR5/6	9.66
	02	4–10	7.5YR4/4	10YR6/6	9.67
	03	10–14.5	7.5YR4/4	10YR6/6	8.78
	04	14.5–17	7.5YR4/3	10YR5/4	9.09
	05	17–20.5	7.5YR2.5/2	10YR5/4	9.49
	06	20.5–23	2.5Y3/3	10YR5/3	11.17
	07	23–24.5	2.5Y2.5/1	2.5Y5/3	8.72
	08	24.5–28	2.5YR4/3	2.5Y6/4	7.39
	09	28–29.5	5YR4/6	5YR6/8	4.54
	10F	29.5–32	10YR8/6	10YR8/4	11.36
	11A	32–34?	7.5YR5/6	10YR7/4	11.54
	11F	–	–	–	–
GL-03	01	0–3	10YR3/2	10YR4/4	11.72
	02	3.5–5	5Y4/1	10YR5/1	15.38
	03	5–5.5	5Y7/1	10YR6/1	–
	04	5.5–6	5Y6/1	10YR6/1	18.57
	05	6–7	5Y5/1	2.5YR5/1	20.62
	06	7–10.5	5Y4/1	2.5YR6/1	14.81
	07	10.5–14	5Y3/1	2.5YR5/1	17.59
	08	14–17	5Y2.5/1	2.5YR5/1	21.50
	09	17–21	5Y4/1	2.5YR6/1	14.99
	10	21–24	5Y4/1	2.5YR6/1	15.88
	11	24–27	5Y4/1	2.5YR6/1	1.29
	12	27–31	5Y3/1	2.5YR5/1	13.93
GL-04	01	0–2	7.5YR3/4	7.5YR5/6	14.47
	02	2–6	7.5YR4/6	7.5YR6/6	15.52
	03	6–7.5	7.5YR5/6	7.5YR6/6	–
	04	7.5–9.5	7.5YR6/6	7.5YR6/6	4.19
	05	9.5–13	10YR7/6	10YR7/6	3.40
	06	13–17.5	10YR7/6	10YR7/6	2.15
	07	17.5–20	10YR6/6	10YR5/6	9.28
	08	20–22.5	10YR5/6	10YR6/6	5.15

Table 2. Continued.

Core	Sample Number	Depth (cm)	Color		LOI (%)
			moist	dry	
GL-05	01	0–3	7.5YR4/6	5YR6/6	–
	02	3–4.5	5YR4/6	5YR6/6	15.32
	03	4.5–6.5	7.5YR5/6	7.5YR5/6	6.92
	04	6.5–9.5	2.5YR4/6	5YR5/8	7.90
	05	9.5–12	2.5YR4/6	5YR5/8	6.12
GL-06	01	0–3.5	7.5YR6/6	10YR6/4	19.15
	02	3.5–6.5	5Y2.5/1	10YR4/1	20.63
	03	6.5–8.5	10YR5/4	10YR7/4	19.53
	04	8.5–10	5Y3/2	10YR5/2	21.43
GL-07	01	surface	7.5YR4/4	7.5YR4/4	16.20
GL-08	01	0–3.5	5YR5/6	7.5YR5/6	10.18
	02	3.5–9	5YR5/6	5YR6/6	6.65
	03	9–10.5	5YR4/6	7.5YR5/6	7.75
	03a	10.5–11	5YR5/4	7.5YR5/4	5.13
	04	11–17	2.5YR4/6	7.5YR5/6	8.27
	05	17–20	2.5YR4/6	7.5YR6/6	7.57
	06	20–23	5YR4/6	7.5YR6/6	7.38
	07	23–27	5YR4/6	7.5YR6/6	7.63
	08	27–29	2.5YR4/6	7.5YR6/6	7.81
	09	29–31	2.5YR4/6	7.5YR5/6	7.47
	10	31–34	5YR4/6	7.5YR5/4	8.49
	11	34–36	5YR4/6	7.5YR6/6	8.06
	12	36–39	5YR4/6	7.5YR6/6	7.17
13	39–42.5	2.5YR4/6	7.5YR6/6	7.07	
GL-09	01	0–5	7.5YR7/4	7.5YR8/2	20.77
	02	5–9	2.5YR6/6	5YR8/3	22.63
	03	9–12	10R6/6	5YR7/4	23.81
	04	12–16.5	10R6/6	5YR6/4	23.40
	05	16.5–20	10R6/4	5YR8/3	23.29
GL-10	01	0–5	5YR8/3	5YR7/3	12.64
	01a	–	–	–	–
	02	5–10	5YR8/3	5YR8/3	3.07
	03	10–15.5	5YR6/3	5YR7/3	9.72
	03a	–	–	–	–
	04	15.5–21	5YR5/4	5YR7/3	12.13
	05	21–27	5YR4/4	5YR6/3	12.17
	06	27–31	2.5YR4/6	5YR6/3	12.74
	07	31–35	2.5YR4/4	2.5YR6/4	7.58
	07a	–	N9	N9	–
08	35–36	5Y5/3	10R6/4	10.75	
09	36–40	2.5YR4/3	5YR7/3	5.17	
GL-11	01	0–6	2.5YR6/8	5YR7/4	4.02
	02	6–12	2.5YR6/8	5YR7/4	4.84

Table 3. Percentage values of the different textural parameters of sediments from Pirata-Pont-Piqueta system.

Core	Sample Number	Gravel (%)	Sand					Silt (%)	Clay (%)
			VCS (%)	CS (%)	MS (%)	FS (%)	VFS (%)		
PP-00	01	85.00						5.00	?
	02	60.00						25.00	?
PP-01	01	0.00	0.40	5.50	17.10	18.30	18.90	32.68	7.12
	02	0.00	0.68	7.20	17.80	13.00	14.80	35.10	11.40
	03	0.00	0.94	6.10	14.40	10.20	5.00	39.60	23.30
	04	0.00	0.00	0.00	0.06	0.40	1.50	81.40	16.60
	05	0.00	0.00	0.00	0.24	2.60	7.90	78.30	11.00
PP-02	01	0.00	0.00	0.00	0.00	2.11	13.90	69.30	14.70
	02	0.00	0.20	3.00	10.40	11.70	13.50	50.80	10.40
	03	0.00	3.98	18.40	16.40	6.60	9.30	35.20	10.10
	04	0.00	0.00	0.11	8.10	19.50	21.70	43.52	7.08
	05	0.00	2.90	11.80	22.70	13.70	12.10	32.87	4.34
	06	0.00	0.00	0.35	14.10	27.00	18.90	35.77	3.93
PP-03	01	0.00	0.00	0.00	0.00	0.00	0.00	80.21	19.80
PP-04	01	0.00	0.00	0.00	0.19	2.70	6.00	83.85	7.25
	02	0.00	0.00	0.00	0.12	2.60	7.40	81.17	8.73
PP-05	01	0.00	0.00	0.38	1.60	3.20	2.90	74.30	17.60
	02	0.00	0.00	0.00	0.46	5.40	3.30	72.80	18.00
	03	0.00	0.00	0.00	0.06	4.70	2.50	73.40	19.30
	04	0.00	0.00	0.00	0.01	0.50	2.00	78.20	19.30
PP-06	01	0.00	0.00	0.00	0.01	1.28	3.20	66.50	29.00
	02	0.00	0.00	0.00	0.00	0.00	0.04	52.80	47.20
	03	0.00	0.00	0.00	0.00	0.00	0.00	50.51	49.50
	04	0.00	0.00	0.00	0.00	0.00	0.00	50.41	49.60
	05	0.00	0.00	0.00	0.00	0.00	0.00	39.87	60.10
PP-07	01	0.00	0.00	0.00	0.00	0.00	0.04	84.16	15.80
	02	0.00	0.00	0.00	0.00	0.00	0.67	87.20	12.10
	03	0.00	0.00	0.27	0.70	1.10	4.30	81.90	11.70
	04	0.00	0.00	0.00	0.00	0.00	0.14	85.00	14.90
	05	0.00	0.00	0.07	0.75	1.40	2.80	79.40	15.60
	06	0.00	0.00	0.00	0.93	2.30	3.30	76.90	16.60
	07	0.00	0.00	0.00	0.28	2.00	3.00	80.30	14.40
	08	0.00	0.00	0.00	0.01	0.61	1.60	81.60	16.20
	09	0.00	0.00	0.08	0.16	2.30	3.80	78.40	15.20
	10	0.00	0.00	0.00	0.06	1.80	2.60	77.60	17.90
PP-08	01	0.00	0.00	0.16	0.90	3.20	7.20	75.60	12.90
	02	0.00	0.00	0.00	0.05	2.75	5.20	73.60	18.40
	03	0.00	0.00	0.00	0.00	0.00	0.00	80.75	19.20
	04	0.00	0.00	0.00	0.01	0.61	2.30	79.30	17.80
	05	0.00	0.00	0.00	0.42	1.80	3.70	76.00	18.10
	06	0.00	0.00	0.00	0.04	1.63	2.70	77.10	18.50
	07	0.00	0.00	0.00	0.00	0.00	0.00	80.30	19.70

Table 3. Continued.

Core	Sample Number	Gravel (%)	Sand					Silt (%)	Clay (%)
			VCS (%)	CS (%)	MS (%)	FS (%)	VFS (%)		
PP-08bis	08	0.00	0.00	0.00	0.43	2.80	2.50	77.10	17.20
	09	0.00	0.00	0.00	0.11	2.05	3.50	78.00	16.30
	10	0.00	0.00	0.01	2.23	7.60	5.50	70.90	14.00
	11	0.00	0.00	0.00	0.00	0.00	0.00	81.27	18.70
PP-09	01	0.00	0.00	0.00	0.00	0.00	0.00	61.18	38.80
PP-11	01	0.00	0.00	0.00	0.44	8.90	17.80	67.44	5.46
PP-12	01	0.00	0.00	11.80	38.50	16.90	11.60	18.57	2.63
	02	0.00	0.00	3.60	15.60	17.10	20.50	36.73	6.47
	03	0.00	0.77	6.80	12.90	7.80	14.30	50.40	7.31
	04	0.00	0.55	5.08	8.90	4.80	19.60	56.71	4.39

Table. 4. Percentage values of the different textural parameters of sediments from Cova de sa Gleda.

Core	Sample Number	Gravel (%)	Sand					Silt (%)	Clay (%)	
			VCS (%)	CS (%)	MS (%)	FS (%)	VFS (%)			
GL-01	01	0.00	0.00	0.00	0.00	0.00	0.00	0.01	53.29	46.70
	02	0.00	0.00	0.00	0.00	0.00	1.20	5.80	53.50	39.50
	03	0.00	0.00	0.00	0.00	0.00	0.00	0.00	50.30	49.70
	04	0.00	0.00	0.00	0.00	0.00	1.00	1.90	46.80	50.30
	05	0.00	0.00	0.00	0.00	0.00	1.00	2.20	55.20	41.60
	06	0.00	0.00	0.00	0.00	0.00	1.10	6.30	53.80	38.80
	07	0.00	0.00	0.00	0.00	0.00	0.60	6.60	56.80	36.00
	08	0.00	0.00	0.00	0.00	0.00	0.20	1.80	49.50	48.50
	09	0.00	0.00	0.00	0.00	0.00	0.00	1.50	54.60	43.90
	10	0.00	0.00	0.00	0.00	0.00	2.00	6.80	64.60	26.60
	11	0.00	0.00	0.00	0.00	0.00	0.00	2.00	52.80	45.20
	12	–	–	–	–	–	–	–	–	–
	13	0.00	0.00	0.00	0.80	3.90	7.50	–	53.60	34.20
	14	0.00	0.00	0.00	0.00	0.30	2.10	–	55.10	42.50
	15	0.00	0.00	0.00	0.00	0.10	1.80	–	47.50	50.60
GL-02	01	0.00	0.00	0.00	0.00	0.30	5.90	51.80	42.00	
	02	0.00	0.00	0.00	0.00	0.20	3.10	57.00	39.70	
	03	0.00	0.00	0.00	0.00	0.00	3.30	51.30	45.40	
	04	0.00	0.00	0.00	0.00	1.10	2.00	50.60	46.30	
	05	0.00	0.00	0.00	0.00	0.70	3.40	55.40	40.50	
	06	0.00	0.00	0.00	0.00	2.20	11.80	59.70	26.30	
	07	0.00	0.00	0.00	0.00	2.00	9.20	64.30	24.50	
	08	0.00	0.00	0.00	0.00	0.30	5.60	56.20	37.90	
	09	0.00	0.00	0.00	0.00	0.10	1.60	52.10	46.20	
	10F	0.00	0.00	0.00	0.00	0.20	1.00	67.20	31.60	
	11A	–	–	–	–	–	–	–	–	–
11F	0.00	0.00	0.00	0.00	0.00	1.00	69.90	29.10		
GL-03	01	0.00	0.00	0.00	0.00	2.50	17.30	70.90	9.30	
	02	0.00	0.00	0.00	0.00	2.70	19.00	69.20	9.10	
	03	0.00	0.00	0.00	0.00	6.00	25.40	60.50	8.10	
	04	0.00	1.70	4.50	9.90	14.80	26.00	39.37	3.73	
	05	0.00	0.00	0.00	0.00	6.40	28.20	57.60	7.80	
	06	0.00	0.00	0.00	0.10	8.00	30.30	53.19	8.41	
	07	0.00	0.00	1.10	9.10	20.00	22.70	40.25	6.85	
	08	0.00	3.60	14.80	22.90	15.20	14.00	25.59	3.91	
	09	0.00	0.00	0.00	0.10	10.60	31.10	50.29	7.91	
	10	0.00	0.00	0.10	3.60	15.30	26.60	46.83	7.57	
	11	0.00	0.00	0.40	7.60	19.80	23.40	42.52	6.28	
	12	0.00	0.00	0.40	8.80	19.80	23.50	41.61	5.89	
GL-04	01	0.00	0.00	0.30	4.20	14.50	27.10	46.72	7.18	
	02	0.00	0.00	0.00	0.00	5.90	24.50	61.13	8.47	
	03	0.00	0.00	0.00	0.10	7.40	24.00	61.27	7.23	
	04	0.00	3.60	9.70	16.70	12.90	16.40	36.22	4.48	
	05	0.00	1.10	9.60	16.60	17.50	18.50	34.68	2.02	
	06	0.00	0.00	3.20	14.80	24.80	23.10	31.87	2.23	
	07	0.00	0.20	1.30	6.30	11.00	25.60	50.75	4.85	
	08	0.00	1.60	5.00	7.00	11.90	25.40	44.44	4.66	

Table 4. Continued.

Core	Sample Number	Gravel (%)	Sand					Silt (%)	Clay (%)
			VCS (%)	CS (%)	MS (%)	FS (%)	VFS (%)		
GL-05	01	–	–	–	–	–	–	–	–
	02	0.00	0.00	0.00	0.00	4.90	17.50	67.00	10.60
	03	19.13	21.44	21.47	16.88	9.94	1.48	3.48	0.32
	04	0.00	0.00	0.00	0.00	4.50	19.40	67.95	8.15
	05	0.00	0.00	0.00	0.00	2.60	15.60	73.15	8.65
GL-06	01	0.00	0.90	4.80	10.10	15.00	22.00	41.31	5.89
	02	0.30	11.00	23.00	18.10	10.40	10.90	23.36	2.94
	03	0.00	0.00	1.30	10.10	18.80	24.10	39.70	6.00
	04	0.00	3.50	13.00	18.10	14.80	14.90	31.41	4.29
GL-07	01	0.00	0.00	0.00	1.80	5.10	7.40	49.30	36.40
GL-08	01	0.00	0.00	0.00	0.00	2.60	19.80	69.24	8.36
	02	0.00	0.00	0.00	0.00	5.50	26.80	60.30	7.40
	03	0.00	0.00	0.00	0.00	2.10	19.20	69.45	9.25
	03a	0.00	0.00	0.00	0.00	1.90	22.90	67.80	7.40
	04	0.00	0.00	0.00	0.00	5.10	25.90	61.36	7.64
	05	0.00	0.00	0.00	0.00	2.90	23.30	65.81	7.99
	06	0.00	0.00	0.00	0.00	4.10	23.90	63.63	8.37
	07	0.00	0.00	0.00	0.00	4.40	25.10	62.10	8.40
	08	0.00	0.00	0.00	0.00	1.60	17.90	70.60	9.90
	09	0.00	0.00	0.00	0.00	1.60	17.50	70.50	10.40
	10	0.00	0.00	0.10	3.10	9.60	22.10	56.18	8.92
	11	0.00	0.00	0.00	0.00	5.30	21.00	64.75	8.95
	12	0.00	0.00	0.00	0.00	1.30	16.80	71.97	9.93
13	0.00	0.00	0.00	0.00	2.90	21.50	66.41	9.19	
GL-09	01	0.00	0.50	5.10	9.60	8.20	14.10	51.50	11.00
	02	0.00	1.90	8.90	11.10	7.60	14.20	47.32	8.98
	03	0.00	0.00	0.60	5.20	6.70	21.30	56.62	9.58
	04	0.00	0.00	0.50	3.70	7.90	23.30	55.73	8.87
	05	0.00	0.00	1.10	8.60	7.20	18.10	55.83	9.17
GL-10	01	–	–	–	–	–	–	–	–
	01a	–	–	–	–	–	–	–	–
	02	–	–	–	–	–	–	–	–
	03	–	–	–	–	–	–	–	–
	03a	–	–	–	–	–	–	–	–
	04	–	–	–	–	–	–	–	–
	05	0.00	0.00	0.20	5.10	11.80	26.40	51.06	5.44
	06	–	–	–	–	–	–	–	–
	07	–	–	–	–	–	–	–	–
07a	–	–	–	–	–	–	–	–	
08	0.00	0.00	0.00	0.00	6.60	28.50	58.56	6.34	
09	–	–	–	–	–	–	–	–	
GL-11	01	0.00	14.16	37.30	18.60	7.80	3.40	10.48	8.26
	02	0.00	6.20	28.30	26.41	11.80	5.50	12.60	9.19

Table 5. Textural statistical parameters of sediments from Pirata-Pont-Piqueta system.

Core	Sample Number	Mean (μm)	Median (μm)	m/M	Mode (μm)	S.D. (μm)	Skewness
PP-00	01						
	02						
PP-01	01	161.80	94.77	1.71	170.80	188.20	1.86
	02	168.00	74.32	2.26	361.80	216.00	1.88
	03	134.50	10.72	12.55	291.90	223.30	2.28
	04	12.44	7.78	1.61	10.52	18.67	5.25
	05	27.96	16.14	1.73	30.73	36.05	3.04
PP-02	01	28.64	13.86	2.07	17.98	35.01	1.71
	02	102.90	29.64	3.47	137.80	159.60	2.55
	03	272.90	91.22	2.99	618.40	343.80	1.55
	04	92.35	60.43	1.53	170.80	94.05	1.29
	05	248.70	139.40	1.78	361.80	295.00	1.97
	06	124.60	95.25	1.31	211.60	111.80	1.26
PP-03	01	7.69	5.51	1.40	8.49	6.84	1.37
PP-04	01	29.66	20.90	1.42	27.61	34.58	3.28
	02	27.92	17.12	1.63	27.61	34.29	2.95
PP-05	01	24.30	6.28	3.87	6.85	62.77	4.95
	02	21.66	5.99	3.62	6.85	46.13	3.29
	03	17.71	5.54	3.20	6.85	39.29	3.60
	04	10.23	5.49	1.86	7.63	17.70	5.27
PP-06	01	11.40	4.29	2.65	5.53	24.46	4.53
	02	4.10	2.18	1.88	1.11	5.79	4.33
	03	2.90	2.02	1.43	1.53	2.41	1.52
	04	2.76	2.02	1.37	1.37	2.14	1.18
	05	2.16	1.60	1.35	1.23	1.62	1.34
PP-07	01	11.16	7.73	1.44	10.52	10.73	1.59
	02	15.53	10.52	1.48	11.71	14.58	1.28
	03	23.71	11.10	2.14	10.52	47.69	6.76
	04	12.13	7.84	1.55	9.45	12.14	1.58
	05	18.85	7.60	2.38	9.45	40.20	6.55
	06	20.07	7.58	2.65	9.45	41.58	4.66
	07	17.39	7.93	2.19	9.45	32.63	4.78
	08	11.48	6.40	1.79	8.49	19.20	5.98
	09	17.89	7.15	2.50	8.49	37.98	5.92
	10	13.60	5.88	2.31	7.63	26.53	4.71
PP-08	01	28.06	10.19	2.75	9.45	51.58	4.61
	02	18.97	6.98	2.72	8.49	33.75	3.39
	03	9.09	6.02	1.51	8.49	8.96	1.64
	04	12.76	6.39	2.00	8.49	20.33	5.00
	05	17.26	6.45	2.68	7.63	34.49	4.80
	06	14.14	6.01	2.35	7.63	27.15	4.66
	07	8.13	5.49	1.48	7.63	8.09	1.91
	08	17.85	6.86	2.60	8.49	35.77	4.51

Table 5. Continued.

Core	Sample Number	Mean (μm)	Median (μm)	m/M	Mode (μm)	S.D. (μm)	Skewness
PP-08bis	09	17.35	6.97	2.49	8.49	31.02	4.11
	10	34.55	7.94	4.35	7.63	64.49	2.73
	11	7.08	5.13	1.38	6.16	6.11	1.42
PP-09	01	4.00	2.83	1.41	4.97	3.42	1.35
PP-11	01	48.21	29.12	1.66	38.08	52.59	1.68
PP-12	01	267.60	250.60	1.07	361.80	206.30	0.64
	02	138.70	77.98	1.78	72.46	158.20	1.75
	03	142.90	44.82	3.19	58.48	215.00	2.25
	04	116.00	44.23	2.62	65.10	189.80	2.88

Table. 6. Textural statistical parameters of sediments from Cova de sa Gleda.

Core	Sample Number	Mean (μm)	Median (μm)	m/M	Mode (μm)	S.D. (μm)	Skewness
GL-01	01	7.56	4.36	1.74	4.44	8.98	2.46
	02	15.14	5.65	2.68	4.44	22.57	2.45
	03	6.35	4.03	1.58	4.44	6.81	2.20
	04	8.41	3.87	2.18	4.05	14.29	4.12
	05	14.60	5.42	2.69	4.88	26.76	3.71
	06	17.23	5.76	2.99	4.05	26.37	2.49
	07	17.30	6.64	2.61	4.88	25.08	2.38
	08	8.94	4.16	2.15	4.05	15.43	4.38
	09	9.37	4.70	1.99	4.44	13.49	3.35
	10	22.21	10.48	2.12	12.40	30.10	2.51
	11	9.99	4.56	2.19	4.44	14.39	2.68
	12	–	–	–	–	–	–
	13	26.00	6.90	3.77	4.44	46.65	3.16
	14	10.90	4.93	2.21	4.44	17.41	3.74
	15	8.59	3.94	2.18	4.05	15.66	4.63
GL-02	01	14.96	5.13	2.92	4.05	23.43	2.55
	02	12.29	5.51	2.23	5.36	18.74	3.24
	03	11.38	4.56	2.50	4.05	17.51	2.89
	04	10.90	4.40	2.48	4.05	22.22	4.76
	05	13.35	5.31	2.52	4.44	21.58	3.32
	06	26.92	11.13	2.42	9.37	34.26	1.83
	07	24.78	11.20	2.21	10.29	32.40	2.18
	08	16.77	5.97	2.81	4.44	26.27	2.70
	09	9.88	4.49	2.20	4.05	14.96	3.48
	10F	10.56	7.02	1.50	10.29	13.39	4.26
	11A	–	–	–	–	–	–
11F	11.48	7.32	1.57	9.37	12.73	2.42	
GL-03	01	39.16	31.71	1.24	41.68	33.01	1.21
	02	40.03	31.93	1.25	50.22	33.93	1.13
	03	49.00	39.67	1.24	66.44	40.84	0.97
	04	149.10	75.47	1.98	80.07	216.30	3.26
	05	51.41	42.98	1.20	72.94	41.32	0.80
	06	54.59	46.26	1.18	87.90	44.12	0.75
	07	104.60	70.34	1.49	116.30	113.00	1.79
	08	274.90	166.20	1.65	429.20	294.90	1.63
	09	58.76	49.65	1.18	96.49	46.90	0.66
	10	75.77	54.88	1.38	105.90	78.89	2.19
	11	96.35	65.65	1.47	127.60	99.33	1.68
	12	100.80	68.11	1.48	127.60	103.30	1.71
GL-04	01	78.95	56.49	1.40	96.49	84.13	2.34
	02	48.55	39.28	1.24	60.52	40.36	1.00
	03	50.82	39.66	1.28	55.13	42.91	1.09
	04	208.30	93.59	2.23	429.20	268.50	2.16
	05	195.80	104.90	0.87	127.60	227.20	1.95
	06	145.90	105.10	1.39	140.10	139.40	1.51
	07	90.47	54.91	1.65	66.44	121.10	3.75
	08	135.80	64.57	2.10	87.90	214.80	3.25
GL-05	01	–	–	–	–	–	–

Table 6. Continued.

Core	Sample Number	Mean (μm)	Median (μm)	m/M	Mode (μm)	S.D. (μm)	Skewness
GL-06	02	41.38	3.78	1.35	41.68	38.44	1.31
	03	79.68	46.85	1.70	37.97	95.48	2.45
	04	43.30	33.47	1.29	41.68	37.45	1.26
	05	37.94	29.58	1.28	34.58	32.74	1.37
GL-07	01	136.70	69.29	1.97	105.90	190.60	2.84
	02	438.50	297.30	1.48	567.70	463.00	1.30
	03	108.70	72.35	1.50	116.30	116.20	1.80
	04	246.80	121.70	2.03	471.10	294.90	1.81
GL-08	01	31.82	8.40	3.79	31.50	55.56	2.93
GL-09	01	41.30	33.59	1.23	45.75	33.55	1.07
	02	50.20	41.91	1.20	60.52	39.28	0.87
	03	39.80	32.34	1.23	45.75	32.80	1.07
	03a	43.67	38.74	1.13	50.22	32.15	0.81
	04	49.04	40.78	1.20	60.52	38.73	0.89
	05	44.35	37.05	1.20	55.13	34.84	0.91
	06	46.15	38.00	1.21	55.13	37.10	0.95
	07	47.17	38.97	1.21	60.52	37.69	0.89
	08	38.19	31.35	1.22	45.75	31.52	1.06
	09	37.51	30.28	1.24	41.68	31.50	1.09
	10	62.82	40.28	1.56	55.13	73.95	2.73
	11	45.42	35.73	1.27	45.75	39.16	1.19
	12	37.28	31.28	1.19	45.75	30.24	1.05
13	42.64	35.22	1.21	50.22	34.68	0.99	
GL-10	01	115.10	37.22	3.09	34.58	186.60	2.59
	02	163.30	49.27	3.31	50.22	250.70	2.17
	03	68.63	40.13	1.71	55.13	93.58	2.88
	04	65.26	42.55	1.53	60.52	80.39	2.96
	05	81.10	39.79	2.04	45.75	113.00	2.34
GL-11	01	—	—	—	—	—	—
	01a	—	—	—	—	—	—
	02	—	—	—	—	—	—
	03	—	—	—	—	—	—
	03a	—	—	—	—	—	—
	04	—	—	—	—	—	—
	05	77.20	52.68	1.47	87.90	86.21	2.40
	06	—	—	—	—	—	—
	07	—	—	—	—	—	—
	07a	—	—	—	—	—	—
08	52.28	44.07	1.19	72.94	41.43	0.84	
09	—	—	—	—	—	—	
GL-11	01	557.61	528.94	1.05	684.16	435.23	0.61
	02	410.23	360.78	1.14	517.18	348.29	0.73

Table 7. Semi-quantitative percentages of the mineralogical composition of samples from Pirata-Pont-Piqueta system.

Core	Sample Number	montmorillonita	clh/mont	illite	kaolinite	quartz	feldspars	dolomite	calcite
PP-00	01	0.00	1.77	4.29	2.46	40.81	6.64	i	44.04
	02								
PP-01	01	3.98	0.00	3.04	0.91	14.13	2.17	3.98	71.77
	02	0.00	0.00	1.88	0.00	13.66	0.00	4.71	75.29
	03	0.00	3.19	3.65	3.68	28.99	3.50	11.57	45.41
	04	2.45	0.00	8.55	5.59	70.62	6.02	0.00	6.78
	05	0.00	0.00	5.58	3.67	68.43	13.31	3.87	5.44
PP-02	01	0.00	1.74	3.37	1.09	10.50	0.00	2.47	83.84
	02	0.00	0.00	2.10	2.16	19.89	5.78	1.39	68.78
	03	0.00	0.00	6.73	2.25	13.60	1.26	2.36	73.82
	04	0.00	0.00	6.29	2.34	13.33	1.60	2.68	73.76
	05	0.00	0.00	1.53	0.00	5.10	1.10	0.59	91.69
	06	0.00	0.00	1.43	0.00	3.14	3.49	0.79	91.14
PP-03	01	0.00	0.00	11.98	4.07	66.88	12.71	0.00	4.36
PP-04	01	0.00	3.30	5.99	2.71	64.44	11.60	5.87	6.10
	02	0.00	0.00	4.98	3.16	73.51	13.24	0.00	5.10
PP-05	01	0.00	0.00	10.76	3.86	67.25	10.72	1.76	5.66
	02	0.00	0.00	14.39	6.02	63.12	11.27	0.00	5.19
	03	0.00	0.00	17.91	5.36	59.44	10.71	1.96	4.61
	04	4.24	0.00	13.76	5.51	56.82	12.76	0.00	6.91
PP-06	01	0.00	5.28	14.56	7.74	44.16	10.10	3.43	14.74
	02	0.00	0.00	26.90	10.01	37.35	13.45	5.53	6.77
	03	0.00	4.82	22.43	9.79	39.99	14.40	0.00	8.59
	04	0.00	9.27	22.67	10.30	40.66	12.34	0.00	4.75
	05	0.00	3.08	18.25	11.03	46.38	13.29	0.00	7.96
PP-07	01	0.00	0.00	7.97	5.33	69.70	11.01	0.00	5.98
	02	0.00	0.00	4.34	1.95	75.30	15.91	0.00	2.50
	03	0.00	0.00	7.17	2.41	78.73	8.51	0.00	3.18
	04	0.00	5.15	8.83	2.83	65.89	12.93	0.00	4.36
	05	0.00	2.36	8.44	3.22	70.60	10.34	1.31	3.63
	06	0.00	3.82	8.61	4.14	67.86	10.24	0.00	5.33
	07	0.00	5.21	9.63	4.26	66.27	9.71	0.00	4.92

Table 7. Continued.

Core	Sample Number	montmorillonita	clh/mont	illite	kaolinite	quartz	feldspars	dolomite	calcite
PP-08	08	1.97	0.00	7.23	2.32	68.82	14.73	0.00	5.67
	09	0.00	0.00	10.27	4.86	67.82	10.54	0.00	6.45
	10	0.00	0.00	9.32	4.31	70.47	11.42	0.00	4.38
	01	0.00	0.00	7.09	2.26	76.11	9.86	0.00	4.69
	02	0.00	0.00	13.93	5.59	64.85	12.04	0.00	3.59
	03	0.00	0.00	6.39	2.94	77.98	9.54	0.00	3.15
	04	0.00	0.00	5.21	3.23	72.14	11.81	2.54	5.07
	05	0.00	0.00	8.78	4.63	68.81	13.75	0.00	4.03
	06	0.00	0.00	13.64	4.38	67.16	11.28	0.00	3.53
	07	0.00	0.00	16.86	4.72	66.55	11.88	0.00	0.00
	08	0.00	3.23	10.00	4.92	68.06	10.96	2.82	0.00
PP-08bis									
PP-09	09	0.00	0.47	10.66	4.98	72.49	11.40	0.00	0.00
	10	0.00	0.00	12.00	5.12	73.17	9.72	0.00	0.00
	11	0.00	0.00	15.26	4.55	65.37	11.15	0.00	3.68
PP-10	01	0.00	1.37	21.24	9.01	55.19	8.14	0.00	5.06
	rock rock impurities	0.00 0.00	0.00 0.00	0.00 0.65	0.00 0.00	1.40 99.34	0.00 0.00	0.00 0.00	98.60 0.00
PP-11	01	0.00	0.00	6.76	1.82	76.69	10.26	1.22	3.24
	01	i	0.00	0.91	0.00	12.27	0.00	1.55	85.27
PP-12	02	0.00	0.00	0.00	1.68	8.09	0.00	3.78	86.45
	03	0.00	0.00	1.08	0.00	2.85	0.00	2.67	93.41
	04	0.00	0.00	0.00	0.00	2.28	0.00	0.00	97.72

Table 8. Semi-quantitative percentages of the mineralogical composition of samples from Cova de sa Gleda.

Core	Sample Number	smectite	illite	gypsum	kaolinite	anhydrite	aragonite	quartz	feldspars	calcite	dolomite
GL-01	01	0.00	16.13	0.00	6.42	0.00	0.00	57.84	3.96	9.99	5.66
	02	0.00	14.76	0.00	5.71	11.98	0.00	49.00	7.43	11.12	0.00
	03	2.35	8.72	0.00	2.89	0.00	0.00	63.65	7.49	14.90	0.00
	04	0.00	11.47	0.00	6.25	9.48	0.00	53.45	11.04	8.30	0.00
	05	0.00	9.43	0.00	5.79	6.72	0.00	53.28	7.77	10.88	6.13
	06	0.00	12.03	0.00	7.81	0.00	0.00	58.37	8.86	7.02	5.92
	07	0.00	9.14	0.00	6.08	0.00	0.00	65.34	8.85	6.32	4.27
	08	0.00	12.48	0.00	9.29	0.01	0.00	60.10	8.29	9.82	0.00
	09	0.00	13.91	0.00	7.37	0.00	0.00	60.76	6.39	7.09	4.49
	10	6.47	8.59	0.00	5.41	0.00	0.00	56.74	5.65	8.22	8.91
	11	0.00	17.21	0.00	8.93	6.18	0.00	45.53	7.39	12.33	2.43
	12	0.00	12.03	0.00	5.98	0.00	0.00	54.50	5.98	14.12	7.40
	14	0.00	11.27	0.00	6.25	0.00	0.00	59.83	3.88	12.58	6.19
	15	12.45	12.60	0.00	6.58	4.05	0.00	46.13	4.77	7.98	5.45
	GL-02	01	0.00	17.46	0.00	7.03	0.00	0.00	69.67	0.00	0.00
02		0.00	12.73	0.00	5.27	0.00	0.00	60.27	8.14	6.50	7.08
03		0.00	15.18	0.00	6.07	0.00	0.00	64.40	7.86	6.49	0.00
04		0.00	12.69	0.00	9.05	0.00	0.00	60.88	9.91	7.47	0.00
05		0.00	14.14	2.93	5.77	0.00	0.00	68.41	0.00	8.75	0.00
06		0.00	6.98	0.00	4.32	0.00	0.00	40.40	9.46	32.16	6.68
07		0.00	7.91	0.00	3.67	0.00	0.00	55.10	7.44	12.99	12.89
08		0.00	7.90	0.00	5.48	0.00	0.00	56.72	4.81	15.75	9.34
09		0.00	9.41	0.00	5.75	0.00	0.00	60.75	7.18	9.70	7.21
10F		0.00	5.56	0.00	1.90	0.00	0.00	9.94	4.20	7.94	70.46
11A		0.00	0.00	0.00	0.02	0.00	0.00	0.00	0.00	92.47	7.51
11F	0.00	0.00	0.00	0.00	0.00	0.00	15.58	0.00	30.24	54.18	
GL-03	01	0.00	9.50	4.78	5.63	0.00	0.00	56.86	5.28	17.95	0.00
	02	0.00	3.55	0.00	0.01	0.01	0.00	34.08	4.01	47.84	10.50
	03	0.00	0.00	0.00	0.00	0.00	0.00	16.90	2.11	44.87	36.12
	04	0.00	0.01	0.00	0.00	0.00	0.00	34.83	2.52	41.99	20.65
	05	0.00	7.82	0.00	2.65	0.00	2.90	22.32	3.97	44.12	16.22
	06	0.00	7.79	0.00	2.46	0.00	0.00	24.17	3.48	58.21	3.89
	07	0.00	7.03	0.00	1.65	0.00	0.00	26.88	3.96	57.49	3.00
	08	0.00	6.26	0.00	3.15	3.64	0.00	25.76	9.35	49.90	1.94
	09	0.00	0.01	0.00	0.01	0.00	0.00	24.45	3.91	68.53	3.09
	10	0.00	0.00	0.00	0.00	0.00	0.00	24.85	2.47	69.12	3.55
	11	0.00	3.91	0.00	1.75	0.00	0.00	34.47	2.84	53.43	3.61
	12	0.00	5.10	0.00	0.00	0.00	0.00	31.26	0.00	60.89	2.74
GL-04	01	0.00	9.87	0.00	6.87	4.65	0.00	49.83	6.06	4.55	18.17
	02	0.00	7.73	0.00	4.46	0.01	0.00	30.58	4.30	3.56	49.36
	03	0.00	8.91	0.00	0.02	4.42	0.00	31.42	0.00	17.30	37.94
	04	0.00	1.81	0.00	1.45	0.00	0.00	7.40	0.00	82.35	6.98
	05	0.00	1.58	0.00	0.00	0.00	0.00	3.25	0.00	95.17	0.00
	06	0.00	0.00	0.00	0.00	0.00	0.00	4.32	0.00	95.68	0.00
	07	0.00	17.19	0.00	8.01	0.00	0.00	35.59	5.54	33.67	0.00
	08	0.00	4.86	0.00	2.60	0.00	0.00	8.32	0.00	84.22	0.00
GL-05	01	0.00	1.10	0.00	0.01	0.00	0.00	5.33	0.00	91.31	2.26

Table 8. Continued.

Core	Sample Number	smectite	illite	gypsum	kaolinite	anhydrite	aragonite	quartz	feldspars	calcite	dolomite
GL-06	02	0.00	5.33	0.00	3.61	0.00	0.00	41.49	6.96	9.07	33.54
	03	0.00	1.32	0.00	0.00	0.00	0.00	7.88	0.00	89.48	1.32
	04	0.00	6.97	0.00	3.19	3.23	0.00	72.51	5.66	2.00	6.45
	05	0.00	9.46	0.00	5.11	4.31	0.00	68.62	5.45	7.04	0.00
GL-07	01	0.00	5.16	0.00	3.07	0.00	0.00	61.90	2.24	3.06	24.57
	02	0.00	7.69	0.00	2.34	0.00	0.00	72.85	5.62	6.10	5.40
	03	0.00	6.39	0.00	2.51	0.00	0.00	34.68	5.31	17.41	33.71
	04	0.00	3.74	0.00	3.19	14.68	0.00	51.65	5.67	11.20	9.87
GL-08	01	1.11	3.51	0.00	2.24	0.00	0.00	74.24	7.31	11.59	0.00
GL-09	01	0.00	6.90	0.00	4.19	0.00	0.00	64.64	5.97	18.29	0.00
	02	0.00	16.04	0.00	25.07	0.00	0.00	6.76	18.32	27.10	6.70
	03	0.00	7.33	0.00	3.72	0.00	0.00	58.15	8.88	19.00	2.92
	03a	0.00	5.40	0.00	2.37	0.00	0.00	63.08	2.63	26.52	0.00
	04	0.00	6.98	0.00	4.16	0.00	0.00	67.05	7.01	14.80	0.00
	05	0.00	9.20	0.00	4.78	0.00	0.00	63.77	8.05	14.20	0.00
	06	0.00	11.44	0.00	4.46	0.00	0.00	55.30	9.11	19.69	0.00
	07	0.00	9.62	0.00	4.23	0.00	0.00	56.69	7.44	22.02	0.00
	08	0.00	7.10	0.00	3.55	0.00	0.00	49.26	4.66	29.58	5.86
	09	0.00	9.79	0.00	5.88	0.00	0.00	63.80	7.78	12.74	0.01
	10	0.00	8.64	0.00	4.47	0.00	0.00	61.27	6.25	19.37	0.01
	11	0.00	7.92	0.00	4.75	0.00	0.00	57.66	4.49	25.17	0.01
	12	0.01	7.17	0.00	4.20	0.00	0.00	61.75	4.44	22.44	0.00
13	0.00	8.18	0.00	3.36	0.00	0.00	63.52	4.73	18.27	1.95	
GL-10	01	0.00	0.00	0.00	0.01	0.00	0.00	0.00	0.00	47.90	52.10
	02	0.00	0.01	0.00	0.00	0.00	0.00	5.98	0.00	0.00	94.01
	03	0.00	5.91	0.00	2.54	0.00	0.00	16.07	2.81	0.00	72.66
	04	0.00	5.41	0.00	3.07	0.00	0.00	15.03	0.00	6.08	70.41
	05	0.00	0.01	0.00	0.00	0.00	0.00	12.84	0.00	1.69	85.45
GL-11	01	0.00	4.26	0.00	1.87	0.00	0.00	3.37	0.00	28.36	62.14
	01a	0.00	0.01	0.00	0.00	0.00	0.00	0.00	0.00	4.57	95.42
	02	0.00	0.01	0.00	0.00	0.00	0.00	5.03	0.00	59.42	35.55
	03	0.00	0.01	0.00	0.00	0.00	0.00	4.09	0.00	60.38	35.52
	03a	0.00	0.00	0.00	0.01	0.00	0.00	2.37	0.00	37.49	60.13
	04	0.00	0.01	0.00	0.01	0.00	0.00	4.61	0.00	41.19	54.17
	05	0.00	5.77	0.00	2.67	0.00	0.00	8.14	2.28	17.77	63.37
	06	0.00	8.87	0.00	3.28	0.00	0.00	10.74	0.00	28.62	48.49
	07	0.00	3.58	0.00	2.22	0.00	0.00	9.24	0.00	13.98	70.99
	07a	0.00	0.00	0.00	0.00	0.00	0.00	0.00	0.00	0.00	100.00
GL-11	08	0.00	0.01	0.00	3.84	0.00	0.00	10.37	0.00	62.67	23.10
	09	0.00	3.15	0.00	0.00	0.00	0.00	4.31	0.00	49.72	42.82
GL-11	01	0.00	0.00	0.00	0.00	0.00	0.00	0.47	0.00	85.61	13.92
	02	0.00	0.00	0.00	0.00	0.00	0.00	1.09	0.00	85.52	13.39